molecules

MDPI

Review

Mercury Monohalides as Ligands in Transition Metal Complexes

Matteo Busato [1,2], Jesús Castro [3], Domenico Piccolo [1,4] and Marco Bortoluzzi [1,5,*]

[1] Dipartimento di Chimica, Sapienza Università di Roma, P.le Aldo Moro 5, 00185 Rome, Italy; matteo.busato@uniroma1.it (M.B.); domenico.piccolo@unipd.it (D.P.)
[2] Dipartimento di Scienze Molecolari e Nanosistemi, Università Ca' Foscari Venezia, 30172 Mestre, Italy
[3] Departamento de Química Inorgánica, Facultade de Química, Universidade de Vigo, Edificio de Ciencias Experimentais, 36310 Vigo, Galicia, Spain; jesusc@uvigo.gal
[4] Dipartimento di Scienze Chimiche, Università di Padova, Via Marzolo 1, 35131 Padova, Italy
[5] CIRCC (Consorzio Universitario Reattività Chimica e Catalisi), Via Celso Ulpiani 27, 70126 Bari, Italy
* Correspondence: markos@unive.it; Tel.: +39-0412348561

Abstract: The main categories of transition metal–mercury heterometallic compounds are briefly summarized. The attention is focused on complexes and clusters where the {Hg-Y} fragment, where Y represents a halide atom, interacts with transition metals. Most of the structurally characterized derivatives are organometallic compounds where the transition metals belong to the Groups 6, 8, 9 and 10. More than one {Hg-Y} group can be present in the same compound, interacting with the same or with different transition metals. The main synthetic strategies are discussed, and structural data of representative compounds are reported. According to the isolobality with hydrogen, {Hg-Y} can form from one to three M-{Hg-Y} bonds, but further interactions can be present, such as mercurophilic and Hg···halide contacts. The formal oxidation state of mercury is sometimes ambiguous and thus {Hg-Y} can be considered as a Lewis acid or base on varying the transition metal fragment. Density functional theory calculations on selected Group 6 and Group 9 model compounds are provided in order to shed light on this aspect.

Keywords: mercury; halides; transition metals; organometallic complexes; M-Hg bond

Academic Editor: Michal Szostak

Received: 6 December 2024
Revised: 23 December 2024
Accepted: 23 December 2024
Published: 2 January 2025

Citation: Busato, M.; Castro, J.; Piccolo, D.; Bortoluzzi, M. Mercury Monohalides as Ligands in Transition Metal Complexes. *Molecules* **2025**, *30*, 145. https://doi.org/10.3390/molecules30010145

1. Transition Metal–Mercury Derivatives: General Aspects

Transition metal–mercury complexes were among the first compounds investigated in the field of direct metal–metal bonding. The fact that mercury can be readily attached to a large variety of transition metals has stimulated its use as a building block in the synthesis of mixed-metal clusters. Several examples of coordination and organometallic compounds where mercury formally behaves as a coordinating atom are thus present in the literature. As described in previous reviews [1–5], transition metal derivatives with mercury in the coordination sphere can be cataloged in few main categories.

The first possibility concerns species having general formula L_nM_m-Hg-Hg-M_mL_n, where the {Hg-Hg} group bonds two transition metal fragments. In most cases, the formal oxidation state of mercury is Hg(I). Recent examples are mixed-metal clusters having formulae $[Hg_2\{(C_6Cl_5)_2Pt(\mu\text{-}OH)_2Pt(C_6Cl_5)_2\}_2]^{2-}$ [6] (Figure 1a), $[Hg_2\{Re_7C(CO)_{21}\}_2]^{4-}$ [7] (Figure 1b), $[Hg_2M_2(P_2phen)_3]^{2+}$ [M = Pd, Pt; P_2phen = 2,9-bis-(diphenylphosphino)-1,10-phenanthroline] [8] (Figure 1c) and $[Hg_2\{Pt_3(RNC)_3\}_2(diphos)_3]$ [diphos = 1,5-bis(diphenylphosphino)pentane, 1,6-bis(diphenylphosphino)hexane; RNC = aromatic isocyanide] [9] (Figure 1d). The structure of $[Hg_2\{(C_6Cl_5)_2Pt(\mu\text{-}OH)_2Pt(C_6Cl_5)_2\}_2]^{2-}$ is formally described as two $[(C_6Cl_5)_2Pt(\mu\text{-}OH)_2Pt(C_6Cl_5)_2]^{2-}$ anions bridged by a $[Hg_2]^{2+}$ cation. Each mercury atom interacts with two platinum centers. The Hg-Hg distance

is 2.552(3) Å, comparable with the Hg-Hg bond in mercurous nitrate, 2.5049(6) Å [10]. The Hg-Pt bond lengths are between 2.6629(10) and 2.9865(9) Å. $[Hg_2\{Re_7C(CO)_{21}\}_2]^{4-}$ is composed of two carbidoheptarhenate clusters linked by a $[Hg_2]^{2+}$ cation, with Hg-Hg distance equal to 2.610(4) Å. The six Hg-Re bonds are in the 2.911(3)–2.965(3) Å range. In the Group 10 clusters $[Hg_2M_2(P_2phen)_3]^{2+}$, the phosphine ligands coordinate the zero-valent M centers that interact with a $[Hg_2]^{2+}$ cation [Hg-Pd 2.7419(5)–2.7960(5) Å, Hg-Pt 2.7823(5)–2.8447(6) Å]. $[Hg_2]^{2+}$ is also coordinated by the nitrogen atoms and exhibits Hg-Hg bond lengths comprised between 2.6881(4) Å [M = Pd] and 2.7362(6) Å [M = Pt]. In the $[Hg_2\{Pt_3(RNC)_3\}_2(diphos)_3]$ clusters, the diphosphines bridge two $\{Pt_3(\mu\text{-}RNC)_3\}$ triangles, forming a cage where two mercury atoms are enclosed. The Hg-Hg distances are between 2.826(2) and 2.8424(2) Å, while the Hg-Pt bonds are in the 2.858(3)–2.980(3) range. Different from the previous examples, the mercury centers are considered as zero-valent, which highlights the sometimes ambiguous oxidation state of mercury in transition metal derivatives.

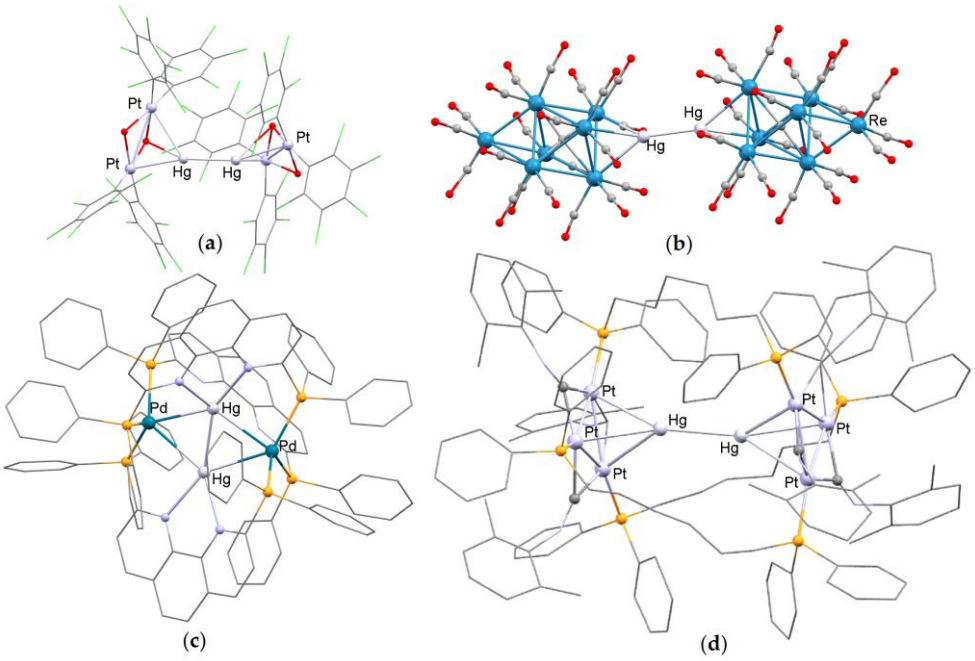

Figure 1. Molecular structures of (**a**) $[Hg_2\{(C_6Cl_5)_2Pt(\mu\text{-}OH)_2Pt(C_6Cl_5)_2\}_2]^{2-}$ [6]; (**b**) $[Hg_2\{Re_7C(CO)_{21}\}_2]^{4-}$ [7]; (**c**) $[Hg_2Pd_2(P_2phen)_3]^{2+}$ [P_2phen = 2,9-bis-(diphenylphosphino)-1,10-phenanthroline] [8]; (**d**) $[Hg_2\{Pt_3(RNC)_3\}_2(diphos)_3]$ [R = 2,6-$Me_2C_6H_3$; diphos = 1,6-bis(diphenylphosphino)hexane] [9]. Color map: Hg, light grey; Pt, light violet; Re, blue; Pd, greenish blue; Cl, light green; P, orange; O, red; N, light blue; C, grey. Hydrogen atoms omitted.

In another group of compounds, a single mercury atom can behave as bridge between two or more transition metals. Selected examples are the trinuclear derivatives $[Hg\{Ni(PNP)\}_2]$ [PNP = pyrrolate-based pincer ligand] [11] (Figure 2a) and $[Hg\{W(\eta^5\text{-}C_5H_5)(CO)_3\}_2]$ [12] (Figure 2b). The Hg-Ni bonds in $[Hg\{Ni(PNP)\}_2]$ are 2.6488(4) and 2.6491(4) Å, while Hg-W distance of 2.7513(3) Å was measured for the two mercury-wolfram bonds in $[Hg\{W(\eta^5\text{-}C_5H_5)(CO)_3\}_2]$. The mercury center can also join transition metal clusters. The structure of $[Hg\{Ru_6C(CO)_{16}\}_2]^{2-}$ is composed of two carbidohexaruthenate fragments, each one forming two Hg-Ru bonds falling in the 2.787(2)–2.902(1) Å range [13]. In $[Hg\{Ru_3(\mu_3\text{-ampy})(CO)_9\}_2]$ [Hampy = 2-amino-6-methylpyridine], two trinuclear ruthenium fragments are connected by a single mercury atom, forming four Ru-Hg bonds with lengths comprised between 2.839(1) and 2.859(1) Å [14]. Ruthenium clusters having formulae $[HgRu_6(CO)_{22}]^{2-}$ (Figure 2c), $[Hg_2Ru_7(CO)_{26}]^{2-}$, $[Hg_3Ru_8(CO)_{30}]^{2-}$ and

$[Hg_4Ru_{10}(CO)_{32}]^{4-}$ were obtained by reacting $[HRu_3(CO)_{11}]^-$ or $[HRu_4(CO)_{12}]^{3-}$ with mercury(II) acetate or chloride [15]. The Hg-Ru bonds vary from 2.6726(13) to 2.9079(10) Å.

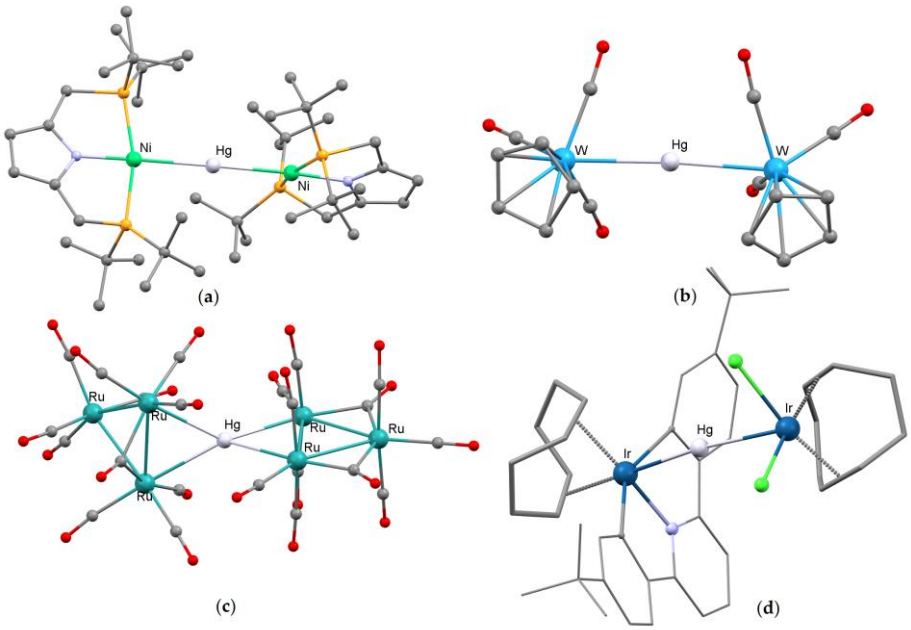

Figure 2. Molecular structures of (**a**) $[Hg\{Ni(PNP)\}_2]$ [PNP = 2,5-bis(di-*tert*-butylphosphanylmethyl)-pyrrolate] [11]; (**b**) $[Hg\{W(\eta^5\text{-}C_5H_5)(CO)_3\}_2]$ [12]; (**c**) $[HgRu_6(CO)_{22}]^{2-}$ [15]; (**d**) [Ir(CˆNˆC)(COD)HgIrCl$_2$(COD)] [H_2CˆNˆC = 2,6-bis(4-*tert*-butylphenyl)pyridine; COD = 1,5-cyclooctadiene] [16]. Color map: Hg, light grey; Ir, dark blue; W, blue; Ru, bluish green; Ni, green; Cl, light green; P, orange; O, red; N, light blue; C, grey. Hydrogen atoms omitted.

Mercury can also bridge transition metals with different coordination spheres. Recent compounds of this type are the polynuclear clusters $[Ir_2Cl_2(\mu\text{-}Cl)_2(COD)_2\{HgIrCl(\kappa^2C,N\text{-}HC\hat{}N\hat{}C)(COD)\}_2]$ and [Ir(CˆNˆC)(COD)HgIrCl$_2$(COD)] (Figure 2d) [H_2CˆNˆC = 2,6-bis(4-*tert*-butylphenyl)pyridine; COD = 1,5-cyclooctadiene]. The first structure can be formally described considering a divalent mercury center between a dinuclear $[Ir_2Cl_2(\mu\text{-}Cl)_2(COD)_2]^{2-}$ cluster and a $[IrCl(\kappa^2C,N\text{-}HC\hat{}N\hat{}C)(COD)]^-$ complex [Hg-Ir bonds 2.6314(3) and 2.5829(3) Å], while in the second compound Hg(II) joins the $[Ir(C\hat{}N\hat{}C)(COD)]^-$ and $[IrCl_2(COD)]^-$ complexes, with Hg-Ir bond lengths equal to 2.5841(3) and 2.6656(3) Å [16]. Finally, mercury can bridge different transition metals. $[Hg_2\{Co_6C(CO)_{12}\}\{W(\eta^5\text{-}C_5H_5)(CO)_3\}_2]^{2-}$ [17] is composed by a carbidohexacobaltate cluster connected to two $\{W(\eta^5\text{-}C_5H_5)(CO)_3\}$ fragments by means of two mercury centers, each one forming three Hg-Co bonds [2.711(2)–2.7261(19) Å] and a Hg-W bond [2.781(2) Å]. In $[\{Re(CO)_4Mo(\eta^5\text{-}C_5H_5)(CO)_2(\mu\text{-}PCy_2)\}Hg\{W(\eta^5\text{-}C_5H_5)(CO)_3\}]$ [Cy = cyclohexyl], mercury joins a dinuclear Re-Mo cluster with a $\{W(\eta^5\text{-}C_5H_5)(CO)_3\}$ fragment [18]. The Hg-M bonds are equal to 2.790(1) Å [M = Re], 2.940(1) Å [M = Mo] and 2.780(1) Å [M = W].

The definition of the most correct formal oxidation state of mercury in heteropolymetallic species is generally not straightforward. Recently, Frenking, Malischewski and co-workers investigated the $[Hg\{Fe(CO)_5\}_2]^{2+}$ (Figure 3a) and $[Hg\{Fe(CO)_4\}_2]^{2-}$ (Figure 3b) trinuclear species, characterized by Hg-Fe distances equal to 2.5745(7) and 2.546(2) Å, respectively [19–21]. According to the energy decomposition analysis with natural orbitals for chemical valence, in both cases the mercury center is best described as Hg(0) instead of Hg(II), thus behaving as a σ-donor toward the iron fragments.

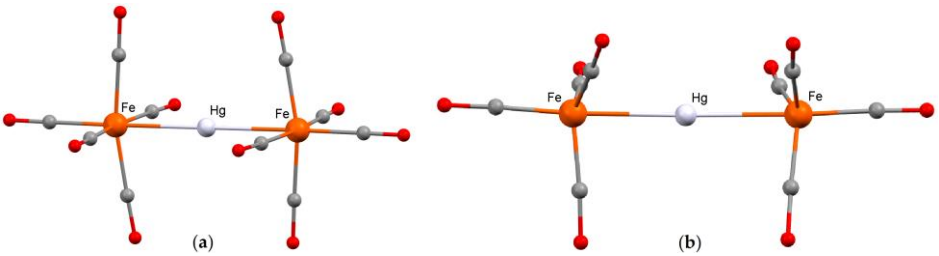

Figure 3. Molecular structures of (**a**) $[Hg\{Fe(CO)_5\}_2]^{2+}$ [19]; (**b**) $[Hg\{Fe(CO)_4\}_2]^{2-}$ [20]. Color map: Hg, light grey; Fe, reddish orange; O, red; C, grey.

The description of clusters containing more than one mercury atom in the structure must also account for mercurophilicity, i.e., the metallophilic interactions possibly occurring among mercury centers, in particular if belonging to the same compound [15,22–25]. Despite the fact that the examples of mercurophilic interactions in the literature are less abundant than those concerning aurophilicity, the possibility of closed-shell Hg(II)···Hg(II) interactions should be taken into account when the Hg···Hg distance is in the range of the Van der Waals contact (about 3.5 Å) or lower. For instance, a dimeric $[Hg_2]^{4+}$ unit with sub van der Waals Hg(II)···Hg(II) distance, 2.820(3) Å, is present in $[Hg_2\{Os_9(C)(CO)_{21}\}_2]^{4-}$ (Figure 4a) [26]. Such a compound derives from the cluster $[Hg_3\{Os_9(C)(CO)_{21}\}_2]^{2-}$ (Figure 4b), where a $[Hg_3]^{6+}$ triangular unit bridges two carbidoennaosmiate fragments. The Hg···Hg(II) distances in the trimercury fragment are comprised between 2.920(7) and 2.931(6) Å [27]. The shortest Os-Hg bond length measured for these clusters is 2.696(5) Å. As another example, the structure of the cation $[Hg_8\{Ir(\eta^5\text{-}C_5Me_5)(CO)\}_6]$ contains a central $\{Hg_4\}$ fragment with Hg···Hg distances between 2.982(2) and 3.0278(18) Å. Each mercury of $\{Hg_4\}$ bonds two iridium centers [28]. The compound also contains two $\{Hg_3\}$ triangles with Hg···Hg distances in the 2.962(2)–3.078(2) Å range.

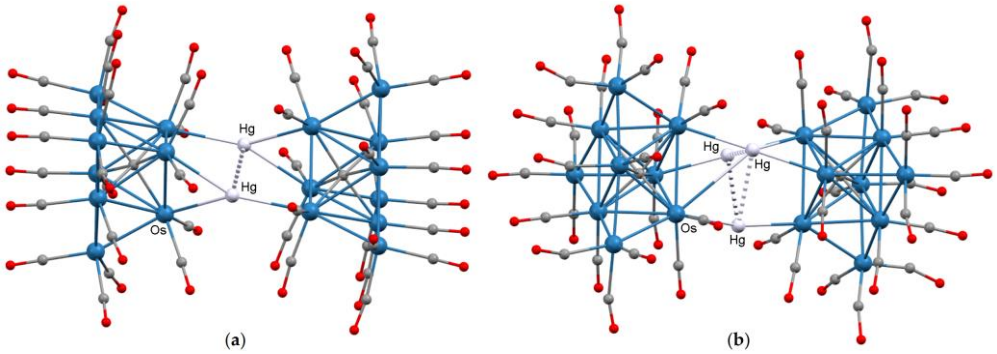

Figure 4. Molecular structures of (**a**) $[Hg_2\{Os_9(C)(CO)_{21}\}_2]^{4-}$ [26]; (**b**) $[Hg_3\{Os_9(C)(CO)_{21}\}_2]^{2-}$ [27]. Color map: Hg, light grey; Os, blue; O, red; C, grey.

In the last category of compounds, mercury is bonded to one or two Y ligands and directly to a metal center, with the formation of species having general formula $L_nM_m\text{-}HgY_y$. The Y ligands can have different nature, according to the typical coordination chemistry of mercury [29–33]. Given the noticeable stability of the Hg-C σ-bonds, transition metal organomercury derivatives were investigated in detail. Mercury is usually bonded to two C-donor fragments that are part of the ancillary ligands surrounding the transition metal. Very short metallophilic interactions between Hg(II) and either Pd(II) or a Group 11 M(I) center were recently observed using quinolin-8-yl fragments able to form Hg-C together with M-N bonds [34]. Figure 5a shows the molecular structure of the Au(I) derivative, characterized by Hg(II)···Au(I) distance equal to 2.596(3) Å. Organomercury-bridged diphosphines are another class of compounds able to form heteropolymetallic complexes with short metal–mercury interactions [35–38]. The structure of a Pd(II) derivative [Hg(II)···Pd(II) 2.9828(6)

Å] is shown in Figure 5b. Two Hg···M interactions can be present in the same molecule if the diphosphine behaves as a bridging ligand, as occurs in the bis(rhodium) complex formed with the ligand (η^5-C_5H_5)Fe($PPh_2C_5H_3$-Hg-$C_5H_3PPh_2$)Fe(η^5-C_5H_5) and in the Au(I) and Au(III) derivatives [{Au(Ar)}$_2${Hg($C_6H_4PPh_2$)$_2$}] and [{$AuCl_2$(Ar)}$_2${Hg($C_6H_4PPh_2$)$_2$}] [Ar = halide-substituted aryls] (see for instance Figure 5c) [39,40]. The Hg···Au(I) distances are between 3.1222(3) and 3.1950(3) Å, while the Hg···Au(III) distances are longer, 3.3973(3) Å. As another example, the reaction of a Cu(I) precursor with a Hg_2N_4-donor macrocycle afforded a heterometallic species with intramolecular Hg···Cu [2.919(7)–2.921(7) Å] and intermolecular Hg···Hg [3.203(4) Å] metallophilic contacts [41,42]. Unsupported interactions between HgR_2 (R = organometallic ligand) and Group 10 or Group 11 transition metal complexes were however reported [43–45]. For instance, in the anion [{$AuHg_2$(*o*-C_6F_4)$_3$}{Hg_3(*o*-C_6F_4)$_3$}]$^-$ the two metallacycles are connected by a short Hg(II)···Au(I) contact, 3.097(2) Å, and the computed interaction energy is around 47.7 kcal mol^{-1} (Figure 5d).

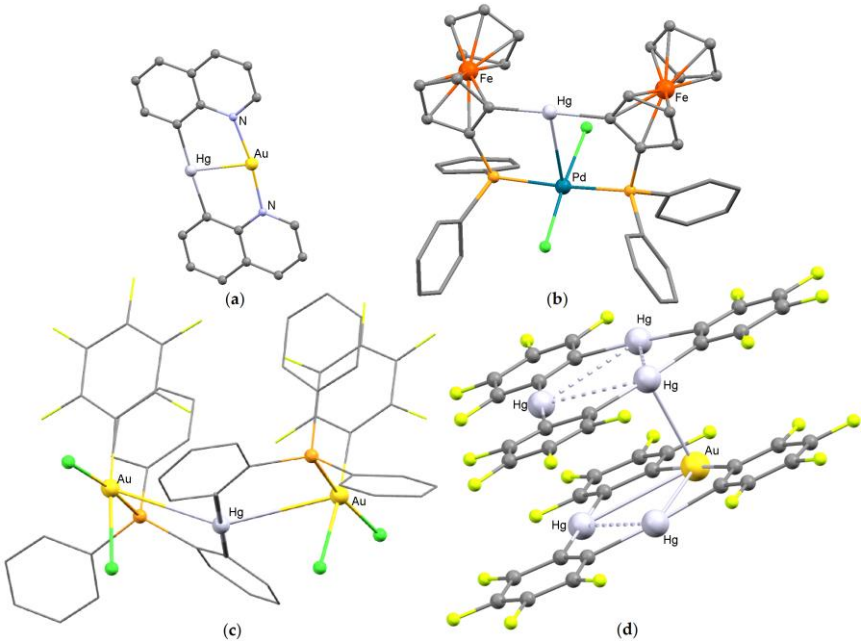

Figure 5. Molecular structures of (**a**) [Au{Hg(C_9H_6N)$_2$}]$^+$ [34]; (**b**) [$PdCl_2$\{Hg($C_5H_3PPh_2$-Fe-C_5H_5)$_2$}] [36]; (**c**) [{$AuCl_2$(C_6F_5)}$_2${Hg($C_6H_4PPh_2$)$_2$}] [40]; (**d**) [{$AuHg_2$(*o*-C_6F_4)$_3$}{Hg_3(*o*-C_6F_4)$_3$}]$^-$ [44]. Color map: Hg, light grey; Au, yellow; Pd, greenish blue; Fe, reddish orange; Cl, light green; P, orange; F, greenish yellow; C, grey. Hydrogen atoms omitted.

2. Heterometallic Transition Metal Complexes with Mercury Dihalides

Divalent mercury halides are among the most common HgY_2 compounds in the chemistry of mercury [46]. The interaction between transition metals in low oxidation state and mercury(II) halides was observed in a number of cases while studying the Lewis basicity of metal carbonyl complexes [47–54]. The synthetic approach was based on the direct reaction of a suitable transition metal carbonyl precursor with HgY_2. Calorimetric measurements on the reaction between Group 6 transition metal carbonyl derivatives and mercury(II) halides in 1,2-dichloroethane solution indicated that the Hg-M bonds formed are at least as strong as the interactions of divalent mercury with conventional Lewis bases. In some cases, the Gibbs energy variation for the reaction is negative by about 7 kcal mol^{-1} [55]. Another reaction pathway involves the formal insertion of metallic mercury in the M-Y bond, even if such a reaction should be considered a redox process. For instance, dinuclear {Fe-HgI_2} complexes with π-acceptor ligands surrounding the iron center were obtained by reacting [FeI_2(CNR)$_4$] [R = alkyl, aryl] with mercury in the

presence of isocyanides and phosphines [56,57]. Yamamoto and co-workers isolated a product having formula $[Ni(HgI_2)(CNR)_4]$ [R = 2,6-$Me_2C_6H_3$] by reacting $[NiI_2(CNR)_2]$ with mercury in the presence of isocyanide. Moreover, the authors assumed the formation of a transient $[Ni(HgI_2)(CNR)_2]$ species while investigating the electrochemical behavior of $[NiI_2(CNR)_2]$ with a mercury electrode [58].

The M-HgY_2 interaction is generally described as a donation of electron density from the transition metal in a low oxidation state, behaving as Lewis base, to HgY_2, which acts as Lewis acid. However, computational studies on $[Ru(M'Cl_2)(CO)_3(PPh_2py)_2]$ [M' = Zn, Cd, Hg; PPh_2py = diphenyl-2-pyridylphosphine] revealed that such an assumption is correct for M' = Zn, while the Ru←M' back-donation is relevant for both M' = Cd and M' = Hg [59].

One of the earliest examples of M-HgY_2 derivatives investigated by means of single-crystal X-ray diffraction is $[Co(HgCl_2)(\eta^5\text{-}C_5H_5)(CO)_2]$ (Figure 6a), showing a Hg-Co bond length equal to 2.578(4) Å. The compound was obtained from $[Co(\eta^5\text{-}C_5H_5)(CO)_2]$ and $HgCl_2$ [60]. It is worth noting that the use of the related isocyanide precursor $[Co(\eta^5\text{-}C_5H_5)\{CNC(O)C_6H_5\}_2]$ afforded a less stable heterobimetallic product [61]. Other species investigated by means of X-ray diffraction are $[Fe(HgI_2)\{CN(p\text{-tolyl})\}_5]$ [Hg-Fe 2.551(1) Å] (Figure 6b) [56] and $[Fe(HgCl_2)(CO)_2(PMe_2Ph)_2\{CS_2C_2(CO_2Me)_2\}]$ [Hg-Fe 2.546(1) Å] (Figure 6c) [62,63]. Structurally characterized examples of trinuclear metal complex showing bridging coordination mode for $HgCl_2$ are $[Pt_2(HgCl_2)Cl_2(dppm)_2]$ (Figure 6d) and $[Rh_2(HgCl_2)(\eta^5\text{-}C_5H_5)_2(\mu\text{-dppm})(\mu\text{-CO})]$ [dppm = bis(diphenylphosphino)methane]. In the first species, the two Hg-Pt bond lengths are between 2.6991(8) and 2.7153(7) Å, contributing to the formation of an "A-frame" structure with $HgCl_2$ at one vertex of the trimetallacycle [64]. Relevant parameters for the trinuclear rhodium derivative are Hg-Rh distances comprised between 2.692(1) and 2.744(2) Å and Hg-Cl bonds comprised between 2.534(3) and 2.581(3) Å [65].

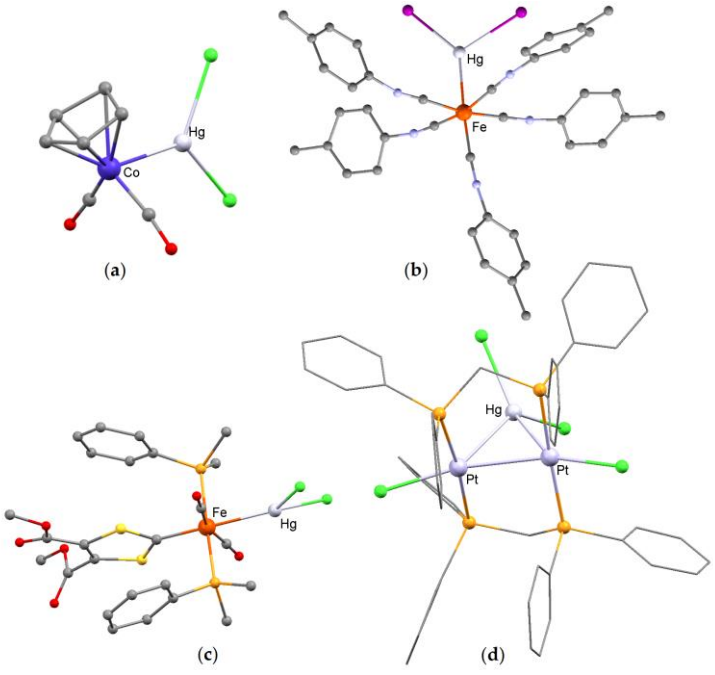

Figure 6. Molecular structures of (**a**) $[Co(HgCl_2)(\eta^5\text{-}C_5H_5)(CO)_2]$ [60]; (**b**) $[Fe(HgI_2)\{CN(4\text{-}MeC_6H_4)\}_5]$ [56]; (**c**) $[Fe(HgCl_2)(CO)_2(PMe_2Ph)_2\{CS_2C_2(CO_2Me)_2\}]$ [62]; (**d**) $[Pt_2(HgCl_2)Cl_2(dppm)_2]$ [dppm = bis(diphenylphosphino)methane] [64]. Color map: Hg, light grey; Pt, light violet; Co, blue; Fe, reddish orange; I, purple; Cl, light green; S, yellow; P, orange; O, red; C, grey. Hydrogen atoms omitted.

HgY_2 can also bond with transition metal clusters through the interaction with halides. For instance, in the structure of $[Pt_2(dppp)_2\{(\mu_3\text{-}Cl)_2HgI_2\}]$ [dppp = 1,3-bis(diphenylphosphino)propane], HgI_2 is connected to the chloro-ligands bridging the Pt centers, and only a weak Hg···Pt interaction [3.1744(4) Å] is present [66].

The bond between the transition metal fragment and HgY_2 can be enforced in the presence of suitable ancillary ligands. For instance, the complex $[Fe(CO)_4(PEtPhpy)]$ [PEtPhpy = 2-(ethylphenylphosphino)pyridine] undergoes an addition reaction with $HgCl_2$ to afford the binuclear derivative $[Fe(HgCl_2)(CO)_4(PEtPhpy)]$ (Figure 7a), where a Hg-Fe bond [2.608(1) Å] is present together with a Hg-N interaction [2.530(4) Å] [67]. In the compound $[Fe(HgI_2)(CO)_3(PPh_2py)_2]$, obtained following the same approach, the interaction between HgI_2 and the transition metal fragment is essentially due to the Hg-Fe bond [2.6780(2) Å], even if two weak mercury–nitrogen interactions are present, the shortest one with Hg-N distance equal to 2.658(2) Å [68]. In related complexes having the general formula $[Fe(HgY_2)(CO)_3(Ph_2Ppym)_2]$ [Y = Cl, Br, I; Ph_2Ppym = 2-(diphenylphosphino)pyrimidine], the Hg-Fe distances are comprised between 2.616(2) and 2.665(2) Å. In the case of Y = Cl, the mercury center weakly interacts with the nitrogen atoms of the pyrimidine rings [Hg-N 2.669(8) and 2.677(9) Å], while only the Fe-Hg bond is present for Y = Br and Y = I [69]. In the Group 8 derivatives $[M(HgI_2)(CO)_3(PPh_2CH_2morph)_2]$ [M = Fe, Ru; PPh_2CH_2morph = *N*-(diphenylphosphinomethyl)morpholine], the M-Hg bonds are 2.665(1) Å [M = Fe] and 2.7075(4) Å [M = Ru]. The shortest Hg-N distances are above 2.7 Å, indicating very weak mercury–nitrogen interactions [70,71]. On the other hand, in the complex $[Pt\{2,6\text{-}(Me_2NCH_2)_2C_6H_3\}\{\mu\text{-}(p\text{-tolyl})NC(H)N(^iPr)\}HgBrCl]$ (Figure 7b) a formamidinate ligand behaves as bridge between a {Pt(NˆCˆN)} fragment and HgClBr. The Hg-N bond length is short, 2.156(11) Å, comparable with the Pt-N(formamidinate) one, 2.155(9) Å. Thanks to the Hg-Pt bond, 2.8331(7) Å, the platinum center assumes a pseudo-square-pyramidal geometry [72].

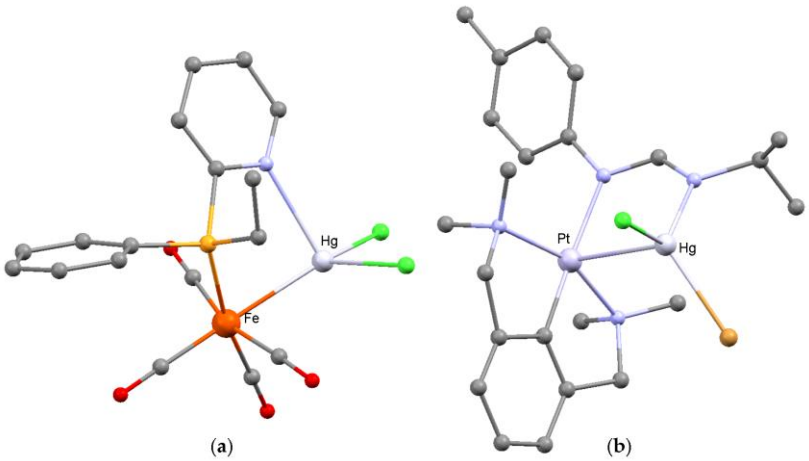

Figure 7. Molecular structures of (**a**) $[Fe(HgCl_2)(CO)_4(PEtPhpy)]$ [PEtPhpy = 2-(ethylphenylphosphino)pyridine] [67]; (**b**) $[Pt\{2,6\text{-}(Me_2NCH_2)_2C_6H_3\}\{\mu\text{-}(p\text{-tolyl})NC(H)N(^iPr)\}HgBrCl]$ [72]. Color map: Hg, light grey; Pt, light violet; Fe, reddish orange; Br, dark orange; Cl, light green; P, orange; O, red; C, grey. Hydrogen atoms omitted.

The formation of a $M_m\text{-}HgY_2$ bond is not the only potential outcome from the reaction between a mercury(II) halide and a transition metal precursor or from the insertion of mercury in the M-Y bond. One of the most common possibilities is the presence in the molecular structure of fragments having general formula $\{Hg_2Y_2(\mu\text{-}Y)_2\}$, which can act as formal terminal ligands [73] or behave as bridges between two transition metal centers, these last connected [74,75] or not [76–78] by a M-M bond. The structures of $[Ir\{Hg(\mu\text{-}Cl)_2HgCl_2\}Cl(CO)(dppm)\{(\mu\text{-}dppm)AuCl\}]$ [Hg-Ir 2.618(3) Å], $[Ru_2\{Hg(\mu\text{-}$

$Cl)_2HgCl_2\}(C_{10}H_8N_2)(CO)_4(P^iPr_3)_2]$ [$C_{10}H_{10}N_2$ = 1,8-diaminonaphthalene; Hg-Ru 2.758(1) and 2.775(2) Å; Ru-Ru 2.827(2) Å] and $[Ni(CNAr)_4\{HgI(\mu\text{-}I)_2HgI\}Ni(CNAr)_4]$ [Ar = 4-Br-2,6-$Me_2C_6H_2$; Hg-Ni 2.619(3) Å] are shown as examples in Figure 8a–c. As for HgY_2, the interaction of $\{HgY(\mu\text{-}Y)_2YHg\}$ with the transition metal fragment can be supported by the coordination of suitable donor groups present in the ancillary ligands, as shown by Zhang and co-workers using 2-pyridylphosphines as bridging ligands between iron carbonyls and mercury [79]. For instance, in the structure of $[Fe\{Hg(\mu\text{-}Cl)_2HgCl_2\}(CO)_4(\mu\text{-}PPh_2py)]$ one of the mercury centers interacts both with iron [Hg-Fe 2.570(2) Å] and with nitrogen [Hg-N 2.483(11) Å]. Hill and Kirk recently provided another example with the arsolyl-complex $[\{HgCl(\mu\text{-}Cl)_2HgCl\}\{Co(\eta^5\text{-}C_4Me_4As)(CO)_2\}_2]$. Two isomers of the compound exist, which differ in the mutual *syn* or *anti* positions of the $\{Co(\eta^5\text{-}C_4Me_4As)(CO)_2\}$ fragments with respect to the rhomboidal $\{HgCl(\mu\text{-}Cl)_2HgCl\}$ core. Besides the Hg-Co bonds [2620(1)–2.6702(9) Å], Hg-As interactions are present, with distances comprised between 2.6334(6) and 2.7268(9) Å [80]. One of the isomers is shown in Figure 8d.

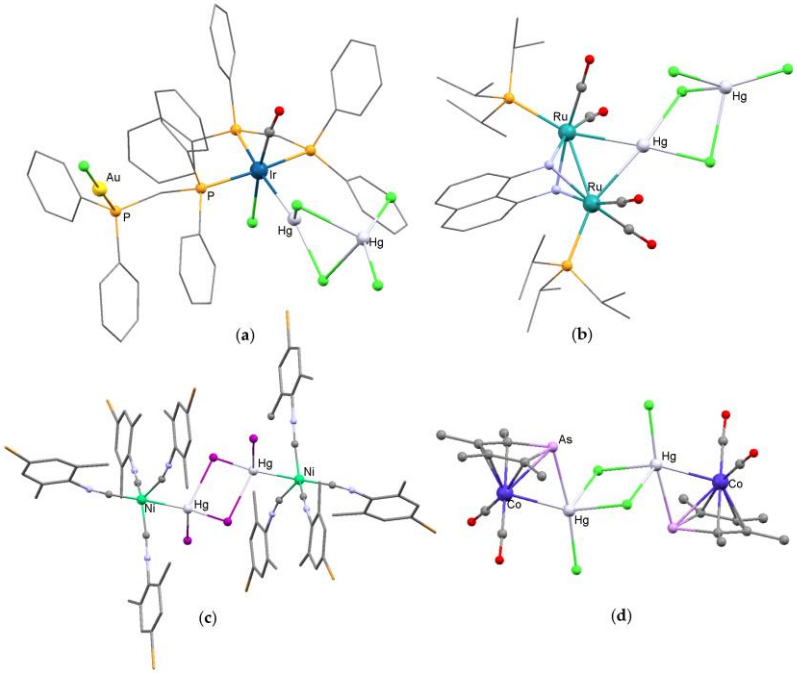

Figure 8. Molecular structures of (**a**) $[Ir\{Hg(\mu\text{-}Cl)_2HgCl_2\}Cl(CO)(dppm)\{(\mu\text{-}dppm)AuCl\}]$ [73]; (**b**) $[Ru_2\{Hg(\mu\text{-}Cl)_2HgCl_2\}(C_{10}H_8N_2)(CO)_4(P^iPr_3)_2]$ [$C_{10}H_{10}N_2$ = 1,8-diaminonaphthalene] [75]; (**c**) $[Ni(CNAr)_4\{HgI(\mu\text{-}I)_2HgI\}Ni(CNAr)_4]$ [Ar = 4-Br-2,6-$Me_2C_6H_2$] [77]; (**d**) $[\{HgCl(\mu\text{-}Cl)_2HgCl\}\{Co(\eta^5\text{-}C_4Me_4As)(CO)_2\}_2]$ [80]. Color map: Hg, light grey; Au, yellow; Ir, dark blue; Ru, bluish green; Ni, green; Co, blue; I, purple; Br, dark orange; Cl, light green; As, violet; P, orange; O, red; C, grey. Hydrogen atoms omitted.

It is worth noting that the nuclearity of the $\{HgY_2\}_x$ fragments can be also higher. The compound $[\{Hg_2(\mu_3\text{-}Cl)_2(\mu\text{-}Cl)_2(HgCl_2)_2\}\{Mo(\eta^6\text{-}C_6H_3Me_3)(CO)_3\}_2]$ (Figure 9a) is composed of two organometallic molybdenum complexes joined by a $\{HgY_2\}_4$ unit. Two of the four mercury centers form Hg-Mo bonds [2.745(1) Å] [81]. The reaction of [Pt(C∧P)(acac)] [C∧P = CH_2-C_6H_4-P(*o*-tolyl)$_2$; acac = 2,4-pentanedionato] with $HgBr_2$ afforded the structurally characterized polynuclear species $[\{Hg_3(\mu\text{-}Br)_4Br_2\}\{Pt(C\wedge P)(acac)\}_2]$ (Figure 9b), where the terminal mercury centers of the trimercury hexahalide fragment form two unsupported Hg-Pt bonds [2.808(1) Å]. The central mercury atom shows an uncommon square-planar environment [82]. The main coordination modes of the $\{HgY_2\}_n$ fragments described in this section are sketched in Scheme 1.

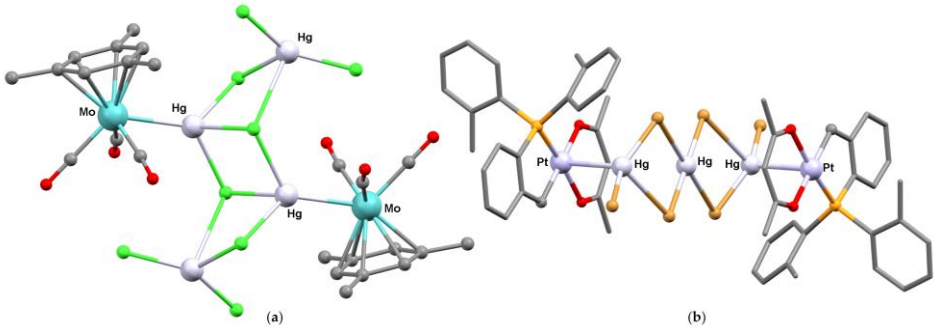

Figure 9. Molecular structures of (**a**) [{$Hg_2(\mu_3\text{-}Cl)_2(\mu\text{-}Cl)_2(HgCl_2)_2$}{$Mo(\eta^6\text{-}C_6H_3Me_3)(CO)_3$}$_2$] [81]; (**b**) [{$Hg_3(\mu\text{-}Br)_4Br_2$}{$Pt(C\wedge P)(acac)$}$_2$] [C∧P = $CH_2\text{-}C_6H_4\text{-}P(o\text{-tolyl})_2$; acac = 2,4-pentanedionato] [82]. Color map: Hg, light grey; Pt, light violet; Mo, light blue; Br, dark orange; Cl, light green; P, orange; O, red; C, grey. Hydrogen atoms omitted.

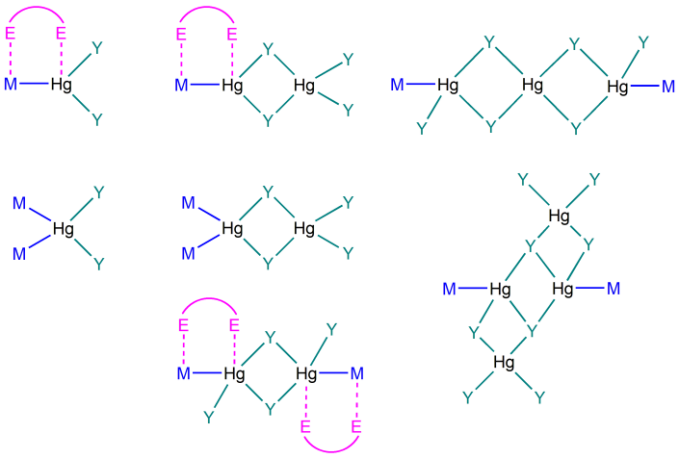

Scheme 1. Sketches of the main coordination modes of the $\{HgY_2\}_n$ fragments (n = 1–4) described in Section 2. Y = halide, E = donor atom.

3. Transition Metal–Mercury Monohalide Derivatives

The apparently simplest cases of transition metal–mercury halide derivatives are species having general formula L_nM_n-HgY, where a mercury monohalide formally behaves as a ligand in the coordination sphere of a transition metal center. Intriguing features are the isolobality of the {HgY} fragment with the hydrogen atom and the possibility of intramolecular {YHg···HgY} or intermolecular {YHg···YHg} interactions (*vide infra*).

As for the L_nM_n-HgY_2 derivatives, a common synthetic approach is based on the reaction of HgY_2 with suitable precursors (Equation (1)); thus, the formation of L_nM_n-HgY instead of L_nM_n-HgY_2 can depend upon the experimental conditions.

$$[L_nM_n] + HgY_2 \rightarrow [L_nM_n\text{-}HgY]Y \quad (1)$$

For instance, on increasing the $[Co(\eta^5\text{-}C_5H_5)(CO)_2]$:$HgCl_2$ ratio, the product isolated was not $[Co(HgCl_2)(\eta^5\text{-}C_5H_5)(CO)_2]$ [60], but a 1:3 adduct whose X-ray structure revealed the presence of $[Co(HgCl)(\eta^5\text{-}C_5H_5)(CO)_2]Cl$ (Figure 10a) and two additional $HgCl_2$ molecules [83]. The cation contains a Hg-Co bond [2.504(9) Å] significantly shorter than that found in $[Co(HgCl_2)(\eta^5\text{-}C_5H_5)(CO)_2]$ [2.578(4) Å]. A short Hg-Cl bond is present [2.348(16) Å] together with other three Hg---Cl contacts, all above 2.8 Å. The {Co-Hg-Cl} fragment is bent, with an angle of 153.5(5)°. As another example, $[Ir(\eta^5\text{-}C_5Me_5)(CO)_2]$ reacts with an excess of $HgCl_2$ to produce the heterometallic complex $[Ir(HgCl)(\eta^5\text{-}C_5Me_5)(CO)_2][HgCl_3]$. Lowering the amount of $HgCl_2$ caused the formation of $[Ir(HgCl_2)(\eta^5\text{-}C_5Me_5)(CO)_2]$ as a secondary product [84]. The X-ray crystal structure of $[Ir(HgCl)(\eta^5\text{-}C_5Me_5)(CO)_2][HgCl_3]$

shows a nearly linear {Ir-Hg-Cl} group [Hg-Ir 2.5870(11) Å, Hg-Cl 2.354(5) Å, Ir-Hg-Cl 172.12(15)°]. Long Hg···Cl interactions [2.914(6)–3.011(5) Å] connect the cation to the $[HgCl_3]^-$ anion.

Other approaches for the synthesis of {M-Hg-Y} derivatives are based on the cleavage of metal–metal bonds by HgY_2, using substrates such as L_nM-Hg-ML_n trinuclear complexes, M-SnR_3 organostannyl species and dinuclear M-M clusters (Equations (2)–(4)) [85–91]. For instance, species having formulae $[M(HgY)(\eta^5\text{-}C_5H_5)(CO)_n]$ [M = Mo, n = 3; M = W, n = 3; M = Fe, n = 2; Y = Br, I] and $[Co(HgY)(CO)_3L]$ [Y = Cl, Br; L = CO or phosphine] were prepared from the corresponding {M-Hg-M} precursors [85,86].

$$[L_nM\text{-}Hg\text{-}ML_n] + HgY_2 \rightarrow 2\,[L_nM\text{-}HgY] \quad (2)$$

$$[L_nM\text{-}SnR_3] + HgY_2 \rightarrow [L_nM\text{-}HgY] + SnYR_3 \quad (3)$$

$$[L_nM\text{-}ML_n] + HgY_2 \rightarrow [L_nM\text{-}HgY] + [L_nM\text{-}Y] \quad (4)$$

The oxidative addition of HgY_2 to a metal center in low oxidation state can also afford {M(HgY)(Y)} complexes (Equation (5)), as shown by the reaction between $[Mo(CO)_4(phen^{Me2})]$ [$phen^{Me2}$ = 2,9-dimethyl-1,10-phenanthroline] and $HgCl_2$, leading to $[Mo(HgCl)Cl(CO)_3(phen^{Me2})]$ [92]. $\{Pt^{IV}(HgY)Y\}$ derivatives prepared through oxidative addition of HgY_2 to divalent platinum complexes are further examples of such a synthetic strategy, deeply investigated by Puddephatt and co-workers [93–96]. Transition metal hydrides can also behave as precursors for the preparation of mercury monohalide derivatives, thanks to the formal exchange between isolobal {HgY} and {H} fragments (Equation (6)). Examples are $[Co(HgY)L_{4\text{-}n}(CO)_n]$ [L = phosphite; n = 0–2] complexes obtained from the corresponding hydrides and HgY_2 [97].

$$[L_nM] + HgY_2 \rightarrow [L_n(Y)M\text{-}HgY] \quad (5)$$

$$[L_nM\text{-}H] + HgY_2 \rightarrow [L_nM\text{-}HgY] + HY \quad (6)$$

Besides $[Co(HgCl)(\eta^5\text{-}C_5H_5)(CO)_2]Cl$ and $[Ir(HgCl)(\eta^5\text{-}C_5Me_5)(CO)_2][HgCl_3]$, several structurally characterized organometallic {M-Hg-Y} derivatives containing a single {HgY} unit are present in the literature, in particular for Group 6 transition metals. In $[Mo(HgCl)(\eta^5\text{-}C_5H_4R)(CO)_3]$ [R = H, Me], the molybdenum center is seven-coordinated, and the Hg-Mo distance is unaffected by the substitution of the cyclopentadienyl ring [2.683(1) Å for R = H, 2.680(2) Å for R = Me]. The Hg-Cl bonds are comprised between 2.442(3) Å [R = H] and 2.398(5) Å [R = Me]. The {Mo-Hg-Cl} fragment is more bent in the cyclopentadienyl derivative [160.02(9)°] with respect to the methylcyclopentadienyl complex [172.0(1)°]. Both the compounds show contacts between {HgCl} fragments belonging to neighboring molecules, with Hg···Cl distances slightly above 3.0 Å [98–100]. $[Mo(HgCl)(\eta^5\text{-}C_5H_4Me)(CO)_3]$ is depicted as an example in Figure 10b. Further analogous compounds with substituted cyclopentadienyl rings were synthesized and characterized, and the interest was focused on the ^{95}Mo and ^{199}Hg chemical shift values [101]. The cyclopentadienyl rings can be formally replaced by isolobal ligands, such as boratabenzenes. The structure of the complex $[Mo(HgCl)(\eta^5\text{-}3,5\text{-}Me_2C_5H_3BN^iPr_2)(CO)_3\}]$ is comparable with that of $[Mo(HgCl)(\eta^5\text{-}C_5H_4Me)(CO)_3]$ [102]. The Mo-Hg bond appears scarcely affected also by the replacement of one of the carbonyl ligands with a trivalent Group 15 ligand. For instance, the Hg-Mo distance in $[Mo(HgI)(\eta^5\text{-}C_5H_4Me)(CO)_2(AsPhMe_2)]$ is

2.685(3) Å, in line with the previous examples. The Hg-I bond length is 2.720(3) Å and the Mo-Hg-I angle is 167.40(8)°. The intramolecular Hg···I distances are long, 3.561(3) Å [103]. The related [W(HgCl)(η^5-C_5H_5)$(CO)_2(PPh_3)$] complex, obtained by reacting [Hg{W(η^5-C_5H_5)$(CO)_3$}$_2$] with PPh_3 in the presence of chlorinated solvents, shows Hg-W and Hg-Cl bond lengths respectively equal to 2.667(1) and 2.382(4) Å and a W-Hg-Cl angle of 173.8(1)° [104]. For what concerns non-cyclopentadienylic Group 6 derivatives, the structures of [Mo(HgCl)Cl$(CO)_3$(N-N)] [N-N = 2,2′-bipyridine, 2,9-dimethyl-1,10-phenanthroline] complexes were reported. The Hg-Mo bond lengths are between 2.700(7) and 2.724(2) Å, slightly longer than in the previously described molybdenum-mercury compounds [92,105].

No {M-Hg-Y} complex of Groups 3 and 4 elements is present in the literature. For what concerns Group 5 derivatives, the proposed general formula for the unique compounds synthesized is [Nb$(HgY)_2$H(η^5-C_5H_5)$_2$]·xHgY_2 [Y = Cl, Br, I; x = 0.5–1], but the characterization data are not supported by X-ray structure diffraction [106]. Crystal structures of dinuclear {M-Hg-Y} compounds belonging to Group 7 are also absent. Despite the fact that complexes of the type [M(HgY)$(CO)_5$] [M = Mn, Re] were prepared from the cleavage of M-Sn or M-Ln^{II} [Ln^{II} = divalent lanthanide] bonds by HgY_2, the characterization data are limited to elemental analyses and IR spectra [90,107]. Only spectroscopic data are available also for the carbonyl complexes [Mn(HgBr)(η^5-C_5H_4Me)$(SiPh_2Me)(CO)_2$] [108], [Re(HgCl)(η^5-C_4H_4BPh)$(CO)_3$] [109] and [Re$(HgY)_2$(η^5-C_5H_5)$(CO)_2$] [Y = Br, I] [110]. As for [Nb$(HgY)_2$H(η^5-C_5H_5)$_2$]·xHgY_2, the last species is described as containing two {HgY} fragments interacting with the same rhenium center. The only technetium derivative reported is [Tc(HgBr)$(NAr)_3$] [Ar = 2,6-diisopropylphenyl] [111], but also in this case the X-ray structure is absent.

An example of a structurally characterized {M-Hg-Y} Group 8 derivative with unsupported Hg-M interaction is *mer*-[Fe(HgBr)$(SiMePh_2)(PMe_3)(CO)_3$]. The Hg-Fe and Hg-Br bond lengths are 2.515(3) and 2.535(3) Å, respectively, and the Fe-Hg-Br angle is 161.0(1)°. The compound is a dimer at the solid state thanks to a second Hg···Br interaction, equal to 3.063(1) Å [112]. The compounds [{Fe(HgY)$(CO)_4$}Hg{Fe(HgY)$(CO)_4$}] [Y = Cl, Br] [113] allow the comparison between the Hg-M bonds involving {HgY} and {μ-Hg} fragments in the same molecule. The interactions of the iron centers with the bridging mercury atom are longer [2.562(2)–2.570(2) Å for Y = Cl; 2.637(3)–2.638(4) Å for Y = Br] than those with the mercury monohalides, in particular when Y = Br [2.518(2)–2.522(2) Å for Y = Cl; 2.351(3)–2.385(3) Å for Y = Br]. The structure of [{Fe(HgBr)$(CO)_4$}Hg{Fe(HgBr)$(CO)_4$}] is depicted in Figure 10c. Besides the Hg-Y bonds, in both the structures additional Hg···Y long interactions are present, above 3.1 Å. Another noticeable example of iron–mercury complex is [Fe$(HgCl)_2(CO)_4$], discovered in 1928 [114], where two {HgY} fragments interact with the same transition metal center. The structure of the related [Fe$(HgBr)_2(CO)_4$] complex (Figure 10d) revealed the presence of mercurophilic interaction between the *cis*-{HgBr} fragments, with Hg···Hg distance around 3.0–3.1 Å [115]. One or two carbonyl ligands of [Fe$(HgY)_2(CO)_4$] can be replaced by N-donor ligands [53]. The synthesis and reactivity of other {Fe-Hg-Y} complexes are reported in the literature, such as [Fe(HgY)(NO)$(CO)_3$] [116] and [Fe(HgY)(η^5-C_5H_5)$(CO)_2$] [90,117,118], but unfortunately data from single-crystal X-ray diffraction were not collected. Bond lengths and angles are instead available for the osmium derivative [Os(HgCl)(NO)$Cl_2(PPh_3)_2$], formed by oxidative addition of $HgCl_2$ to [OsCl(CO)(NO)$(PPh_3)_2$] and loss of the carbonyl ligand. The transition metal center is six-coordinated and the Hg-Os distance is 2.577(6) Å. The {Os-Hg-Cl} fragment is almost linear, being the angle 177(1)° [119].

Besides [Co(HgCl)(η^5-C_5H_5)$(CO)_2$]Cl [83] and [Ir(HgCl)(η^5-C_5Me_5)$(CO)_2$][$HgCl_3$] [84], examples of structurally characterized Group 9 {M-Hg-Y} complexes are [Co(HgY){$P(OPh)_3$}$_4$]

[Y = Cl, Br] derivatives [120]. The Hg-Co distance is almost unaffected by the choice of the halide, falling in the 2.481(2)–2.485(2) Å range. The Co-Hg-Y angles are also strictly comparable, being 163.1(1) and 163.8(1)°. Unfortunately, the bond lengths and angles are not available for the related tetracarbonyl complexes [121]. In the case of iridium, crystal data were reported for $[Ir(HgCl)Cl_2(CO)(PPh_3)_2]$, dimer at the solid state [Hg-Ir 2.570(1) Å, [Hg-Cl 2.366(5) Å, Hg···Cl 3.148(5) Å, Ir-Hg-Cl 172.2(1)°], and for the isomorphous bromo-derivative $[Ir(HgBr)ClBr(CO)(PPh_3)_2]$, both derived from the oxidative addition of HgY_2 to Vaska's complex *trans*-$[IrCl(CO)(PPh_3)_2]$ [122]. Other compounds have the general formula $[Ir(HgCl)\{CCCW(Tp^{R2})(CO)_2\}_2(CO)(PPh_3)_2]$ [Tp^{R2} = tris(pyrazol-1-yl)borate, tris(3,5-dimethylpyrazol-1-yl)borate]. The Ir-Hg distances are between 2.5905(16) and 2.615(3) Å, while the {Ir-Hg-Cl} fragments are almost linear [123]. A recent example of structurally characterized Group 9–HgCl complex is $[Ir(HgCl)(C^N^C)(COD)]$ [$H_2C^N^C$ = 2,6-bis(4-*tert*-butylphenyl)pyridine] [16]. The Hg-Ir distance is 2.5705(3) Å and the Ir-Hg-Cl angle is 171.64(4)°.

X-ray data for binuclear {M-Hg-Y} compounds with the transition metal center belonging to Group 10 and unsupported M-Hg bonds are available for M = Pd and M = Pt. As described before, $\{Pt^{IV}(HgY)Y\}$ complexes can be obtained from the oxidative addition of HgY_2 to suitable Pt(II) precursors, such as square-planar species with two C-donors and a bidentate N-donor in the coordination sphere [93–96]. The Hg-Pt distance is usually slightly above 2.5 Å and dimerization at the solid state can occur thanks to long Hg···Y interactions. The structure of $[Pt(HgBr)BrMe_2(bpy^{Bu2})]$ [bpy^{Bu2} =4,4′-di(*tert*-butyl)-2,2′-bipyridine] is shown as an example in Figure 10e. $HgCl_2$ also reacts with the trinuclear cluster $[Pt_2Pd(\mu\text{-}dpmp)_2\{CN(2,6\text{-}Me_2C_6H_3)\}_2]^{2+}$ [dpmp = bis(diphenylphosphinomethyl)phenylphosphine], with the break of the Pt-Pd bond and the formation of $[Pt_2Pd(HgCl)(Cl)(\mu\text{-}dpmp)_2\{CN(2,6\text{-}Me_2C_6H_3)\}_2]^{2+}$, where the {HgCl} fragment is bonded to palladium [Hg-Pd 2.5830(5) Å], while the other halide interacts with one of the platinum centers. The mercury–palladium bond was described as Hg^I-Pd^I, and the additional interaction of mercury with one of the platinum atoms is suggested by the Hg···Pt distance equal to 2.8191(3) Å [124]. On considering another synthetic approach, the reaction of $[PtH(PP_3)]^+$ [PP_3 = tris(2-diphenylphosphinoethyl)phosphine] with PhHgCl gave $[Pt(HgCl)(PP_3)]^+$, where the {HgCl} fragment occupies one of the apical positions of a trigonal bipyramid surrounding the platinum center. The Hg-Pt bond length is 2.5511(9) Å and the Pt-Hg-Cl angle is 174.63(7)° [125].

As previously described for HgY_2 and $\{HgY(\mu\text{-}Y)_2YHg\}$, also the interaction of the {HgY} fragment with a transition metal center can be enforced by the presence of donor atoms in the ancillary ligands able to interact with mercury. Functionalized phosphines such as 2-pyridylphosphine, tri(2-furyl)phosphine and related species allowed the preparation of compounds such as $[Ru(HgCl)(PPh_2py)_2(CO)_3][HgCl_3]$, $[Fe(HgI)(CO)_3(Ph_2PQu)_2][HgI_3]$ [PhPQu = 2-diphenylphosphino-4-methylquinoline], $[M(HgCl)Cl_2(CO)(PPh_2py)_2]$ [M = Rh, Ir] and $[Rh(HgCl)(CO)Cl_2\{P(C_4H_3O)_3\}_2]$, where Hg···N or Hg···O interactions support the Hg-M bonds [126–129]. In the *cis*-$[M(HgY)_2(PPh_2py)(CO)_3]$ [M = Ru, Y = Br; M = Os, Y = Cl] derivatives [130], one of the two {HgY} fragments shows an unsupported bond with the transition metal [Hg-Ru 2.602(2) Å; Hg-Os 2.627(1) Å], while the other one also interacts with the nitrogen atom of the pyridine fragment [Hg-Ru 2.628(2) Å, Hg-N 2.772(2) Å; Hg-Os 2.651(1) Å, Hg-N 2.67(1) Å]. Despite this difference, the Hg-Y bonds and M-Hg-Y angles in the same molecule are very similar [Hg-Br 2.540(3) and 2.538(4) Å; Hg-Cl 2.392(6) and 2.400(5) Å; Ru-Hg-Br 165.4(1) and 169.5(1)°; Os-Hg-Cl 177.5(1) and 176.4(1)°]. The structure of the osmium derivative is shown in Figure 11a.

The possibility of quite strong Hg-N interactions with the {M-Hg-Y} fragment is highlighted by the crystal structure of $[Fe\{HgCl(py)\}_2(CO)_4]$, where the Hg center forms bonds with Fe [2.552(8) Å], Cl [2.61(1) Å] and the nitrogen atom of pyridine [2.51(6) Å].

The description of the compound at the solid state must, however, also account for a further intermolecular Hg···Cl interaction equal to 2.771(1) Å [131]. Another example is the triazenido-complex [Ir(HgCl){EtN_3(4-Me-C_6H_4)}$_2$(COD)] [Hg-Ir 2.618(1) Å], where one of the two triazenido-ligands bridges the iridium and mercury centers [Hg-N 2.42(1) Å] (Figure 11b). Mercury also forms an intramolecular [2.41(1) Å] and an intermolecular [3.08(1) Å] Hg-Cl bond [132].

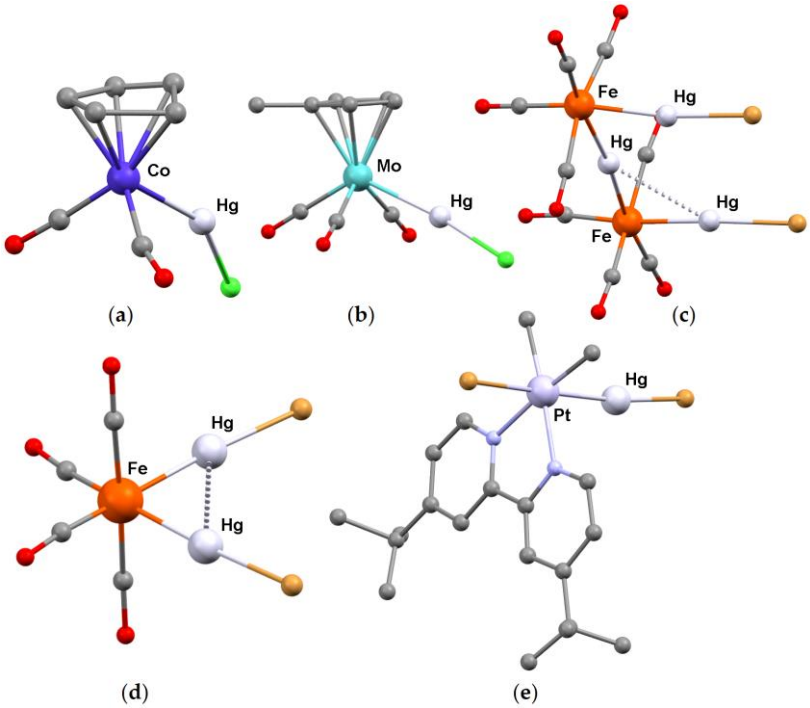

Figure 10. Molecular structures of (**a**) [Co(HgCl)(η^5-C_5H_5)$(CO)_2$]$^+$ [83]; (**b**) [Mo(HgCl)(η^5-C_5H_4Me)$(CO)_3$] [100]; (**c**) [{Fe(HgBr)$(CO)_4$}Hg{Fe(HgBr)$(CO)_4$}] [113]; (**d**) [Fe$(HgBr)_2(CO)_4$] [115]; (**e**) [Pt(HgBr)$BrMe_2$(bpy^{Bu2})] [bpy^{Bu2} =4,4′-di(*tert*-butyl)-2,2′-bipyridine] [95]. Color map: Hg, light grey; Pt, light violet; Mo, light blue; Co, blue; Fe, reddish orange; Br, dark orange; Cl, light green; N, light blue; O, red; C, grey. Hydrogen atoms and intermolecular interactions omitted.

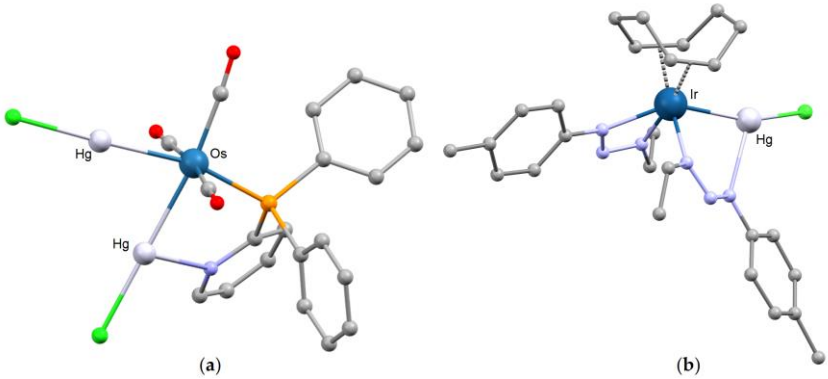

Figure 11. Molecular structures of (**a**) *cis*-[Os$(HgCl)_2$(PPh_2py)$(CO)_3$] [PPh_2py = diphenyl-2-pyridylphosphine] [130]; (**b**) [Ir(HgCl){EtN_3(4-Me-C_6H_4)}$_2$(COD)] [COD = 1,5-cyclooctadiene] [132]. Color map: Hg, light grey; Ir, dark blue; Os, blue; Cl, light green; P, orange; N, light blue; O, red; C, grey. Hydrogen atoms omitted.

{HgY} can formally behave both as a terminal and bridging ligand. For example, treatment of the trinuclear clusters [$Fe_3E(CO)_9$]$^{2-}$ [E = S, Se] with HgI_2 afforded the {HgI}-bridged species [Fe_3(HgI)$E(CO)_9$]$^-$ (Figure 12a, E = S). The mercury center forms in both the cases two almost identical Hg-Fe bonds [2.6384(8) and 2.6385(7) Å for E = S; 2.605(2) and 2.608(2) Å for E = Se]. The Fe-Hg-Fe angles of the metallacycles are be-

tween 64.23(2) and 67.26(6)°, while the Hg-I bonds are between 2.641(1) and 2.6985(4) Å [133,134]. Another Group 8 cluster where {HgY} forms two Hg-M bonds [2.612(3) and 2.862(3) Å] is $[Ru_5C(HgCl)(CO)_{14}(\mu\text{-}Cl)]$, which is reported as a dimer because of the presence of an additional long intermolecular Hg···Cl interaction [2.961(11) Å] in addition to the Hg-Cl bond [2.412(10) Å]. However, the dissociation of the dimer in solution was proposed [13]. The previously described $[Hg\{Ru_3(\mu_3\text{-}ampy)(CO)_9\}_2]$ cluster [14] reacts with $HgBr_2$ to form $[Ru_3(HgBr)(\mu_3\text{-}ampy)(CO)_9]$, where a $\{Ru_2Hg\}$ triangle is present [Hg-Ru 2.735(2) and 2.744(2) Å, Ru-Hg-Ru 63.79(6)°]. Roughly comparable species are the clusters $[Os_3(HgCl)(\mu_3\text{-}C_2Ph_2)(\mu\text{-}Cl)(CO)_9]$ and $[Ru_3(HgBr)(CO)_9(C_6H_9)]$, both showing dimerization at the solid state thanks to intermolecular Hg···Y interactions [135,136]. Dimerization at the solid state is not the only possibility when interactions among {HgY} fragments belonging to different molecules occur. An example is provided by the structure of $[Os_3(HgI)(CO)_{10}(\mu\text{-}\eta^1\text{-}Ph)]$, which is reported as a tetramer. A pseudo-cubic central $\{Hg_4I_4\}$ unit is present in the X-ray structure, where each mercury atom is connected to three iodides [2.9112(8), 2.9645(8) and 3.524(1) Å]. The I-Hg-I angles are 87.29(2) and 91.11(2)°. Moreover, each mercury center forms two Hg-Os bonds [2.7930(6) and 2.7978(7) Å] [137].

Examples of clusters with bridging {HgY} based on metal centers belonging to other Groups are $[Rh_2(HgCl)(\mu\text{-}H)(CO)_2\{\mu\text{-}(PhO)_2PN(Et)P(OPh)_2\}_2]$ [Hg-Rh 2.711(1) and 2.778(1) Å] [138], $[Re_2(HgI)(CO)_8(\mu\text{-}\eta^1\text{-}C_6H_5)]$ [Hg-Re 2.7843(8) and 2.8051(7) Å] [139], $[\{Re_2(HgCl)(CO)_8(\mu\text{-}PCy_2)]$ [Hg-Re 2.777(1) and 2.784(1) Å] and $[\{Re(CO)_4Mo(\eta^5\text{-}C_5H_5)(CO)_2(HgCl)(\mu\text{-}PCy_2)]$ [18]. In the last compound (Figure 12b), there are Hg-Re [2.707(1) Å] and Hg-Mo [2.896(1) Å] bonds and the Re-Hg-Mo angle is 73.6(1)°. Intermolecular Hg···Y interactions at the solid state are common for these species.

Despite the presence of two identical transition metals, the structure of $[RhCl(PPh_3)(CO)(HgCl)(\mu\text{-}pz)_2Rh(CO)(PPh_3)]$ [pz = pyrazolate] is described as a {HgCl} fragment bridging Rh(I) and Rh(III) centers, with Hg-Rh^{I} and Hg-Rh^{III} distances respectively equal to 2.804(3) and 2.586(2) Å [140]. The nature of the M-Hg bonds is a matter of discussion also in trinuclear platinum-mercury derivatives. The compound $[HgBr\{PtMe_2Cl(bpy^{Bu2})\}\{PtMe_2(bpy^{Bu2})\}]$ [95,96] shows a covalent Pt^{IV}-HgBr bond [2.5767(7) Å], but the same {HgBr} fragment is also involved in a second Pt→Hg donor-acceptor interaction with a Pt(II) center [2.6973(4) Å]. Yamaguchi and Yoshiya isolated two coordination isomers of a trinuclear heterometallic derivative having general formula $[HgPt_2(CH_3)_2Cl_4(phen)]_2]$ [phen = 1,10-phenanthroline]. In the first isomer, $[Hg\{PtMe_2Cl(phen)\}_2]$, the mercury atom forms two covalent Hg-Pt bonds [2.5459(8) and 2.5483(7) Å] and the two platinum centers are, including the bonds with mercury, six-coordinated. In the other isomer, $[\{PtMe_2(phen)\}\{HgCl\}\{PtMe_2Cl(phen)\}]$ (Figure 12c), {HgCl} behaves as bridge between two platinum fragments. A covalent bond is present with the six-coordinated platinum [Hg-Pt 2.5744(6) Å], while a longer dative Pt→Hg bond, 2.6635(7) Å, joins a square-planar platinum fragment and {HgCl}, with the formation of a square-pyramidal geometry [141].

{HgY} can also interact with three metal centers of the same cluster, as observable in the structures of $[Ir_6(HgCl)(CO)_{15}]^-$ and $[Ir_6(CO)_{14}(HgCl)_2]^{2-}$ (Figure 13a,b), where one or two faces of the $\{Ir_6\}$ octahedra are capped by {HgCl} fragments, with the formation of three Hg-Ir bonds in the 2.768(2)–2.808(2) Å range [142,143]. Capping {HgY} fragments are present also in the structure of $[Pt_6(HgI)_2(\mu\text{-}CO)_6(\mu\text{-}dppm)_3]$, with Hg-Pt distances varying from 2.770(2) to 2.867(1) Å [144]. A yet more complex situation was observed in the cluster $[\{Hg_2Br_2\}\{Pt_3(HgBr)(\mu\text{-}CO)_3(PPhCy_2)_3\}_2]$ [145], where four {HgBr} fragments are present. Two of them compose a central $\{Hg_2Br_2\}$ square-planar arrangement of two mercury atoms and two bridging bromine atoms, with Hg-Br bond lengths around 2.7 Å. The other two {HgBr} behave as capping ligands toward the two $\{Pt_3\}$ units. Each mercury atom forms three Hg-Pt bonds [Hg-Pt 2.853(1) Å]. The three M-Hg

bonds can have quite different lengths, as in the clusters $[Os_{10}C(HgBr)(CO)_{24}]^-$ [Hg-Os bonds between 2.730(2) and 2.924(2) Å] [146], $[Pd_4(HgBr)_2(CO)_4(PEt_3)_4]$ [Hg-Pd bonds between 2.704(1) and 2.993(1) Å] [147,148], $[Pt_4(HgBr)_2(\mu\text{-}CO)_4(PPh_3)_4]$ [Hg-Pt bonds between 2.736(1) and 3.113(1) Å] [149] and $[Pt_4(HgI)_2(\mu\text{-}CO)_4(PMe_2Ph)_4]$ [Hg-Pt between 2.716(3) and 3.163(3) Å] [150]. The transition metals can be also different, as occurs in the cluster $[Pt_3Ru_6(HgI)(\mu_3\text{-}H)_2(CO)_{21}]^-$, where the mercury center forms two Hg-Ru [2.741(2)–2.774(2) Å] and one Hg-Pt [2.893(1) Å] bonds [151]. The presence of M–M interactions is, however, not mandatory. In $[Rh_3(HgCl)(\mu\text{-}Cl)_3(dpmppp)L_2]^+$ [dpmppp = *meso*-1,3-bis[(diphenylphosphinomethyl)phenylphosphino]propane; L = CO, CN(2,6-$Me_2C_6H_3$)] the three rhodium centers are connected by a tetradentate phosphine, three bridging chloro-ligands and a {HgCl} fragment forming three Hg-Rh bonds in the 2.6408(8)–2.7414(9) Å range [152]. In $[Pt_3(HgCl)(\mu\text{-}OH)_3(C_6F_5)_6]^{2-}$ (Figure 13c), the three platinum atoms are connected by three μ-hydroxo ligands and {HgCl} [Hg-Pt 2.750(1)–2.875(1) Å] [153]. The main coordination modes of {HgY} described in this section are sketched in Scheme 2.

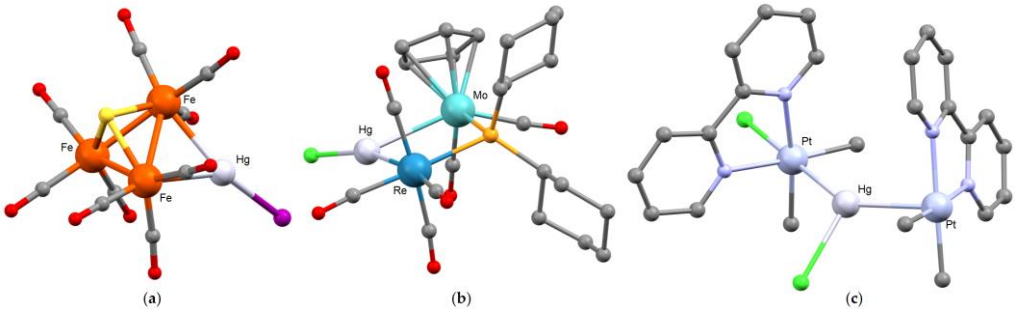

Figure 12. Molecular structures of (**a**) $[Fe_3(HgI)S(CO)_9]^-$ [133]; (**b**) $[\{Re(CO)_4Mo(\eta^5\text{-}C_5H_5)(CO)_2(HgCl)(\mu\text{-}PCy_2)\}]$ [18]; (**c**) $[\{PtMe_2(phen)\}\{HgCl\}\{PtMe_2Cl(phen)\}]$ [phen = 1,10-phenanthroline] [141]. Color map: Hg, light grey; Pt, light violet; Re, blue; Mo, light blue; I, purple; Cl, light green; S, yellow; P, orange; N, light blue; O, red; C, grey. Hydrogen atoms omitted.

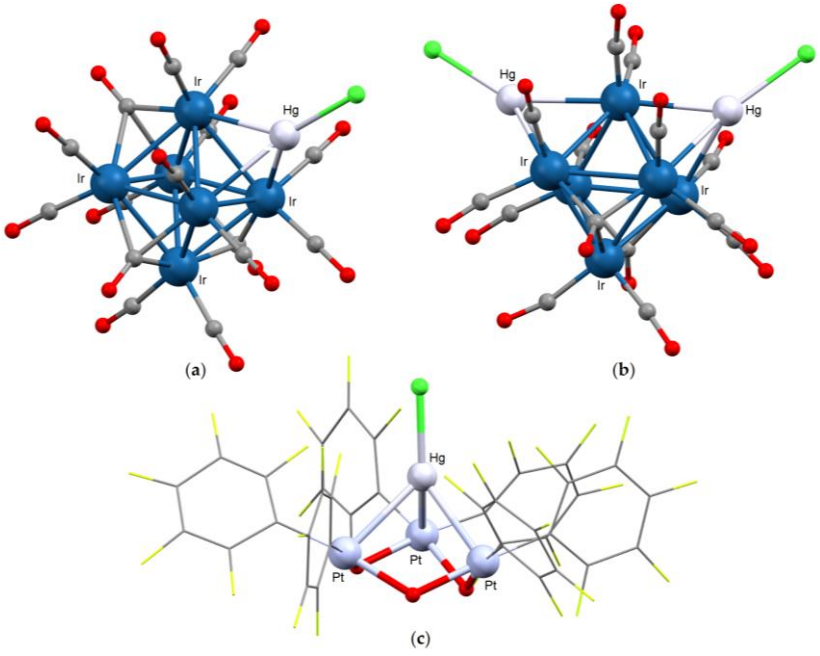

Figure 13. Molecular structures of (**a**) $[Ir_6(HgCl)(CO)_{15}]^-$ [142]; (**b**) $[Ir_6(CO)_{14}(HgCl)_2]^{2-}$ [143]; (**c**) $[Pt_3(HgCl)(\mu\text{-}OH)_3(C_6F_5)_6]^{2-}$ [153]. Color map: Hg, light grey; Pt, light violet; Ir, dark blue; Cl, light green; F, greenish yellow; O, red; C, grey. Hydrogen atoms omitted.

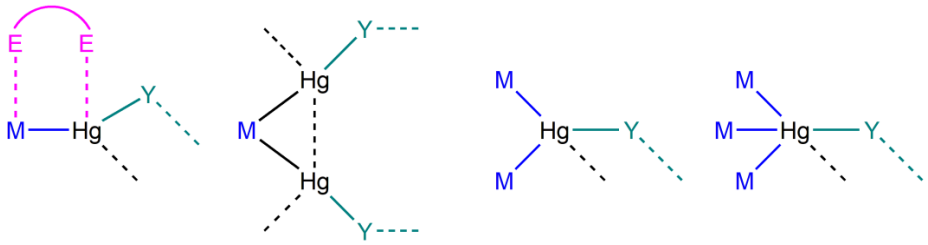

Scheme 2. Sketches of the main coordination modes of {HgY} described in Section 3. Y = halide, E = donor atom.

4. Computational Investigations on {M-Hg-Y} Derivatives

As revealed by the previous examples, the formal oxidation states in transition metal–mercury monohalide derivatives are sometimes ambiguous; thus, the {HgY} fragment can be considered as a Lewis acid or base on varying the transition metal fragment. $[M(HgY)(\eta^5\text{-}C_5H_5)(CO)_3]$ [M = Cr, Mo, W; Y = Cl, Br, I] and $[M(HgY)(\eta^5\text{-}C_5H_5)(CO)_2]^+$ [M = Cr, Mo, W; Y = Cl, Br, I] were selected as model compounds to investigate the M-HgY bonds from a computational point of view. The intermolecular interactions were omitted. Cartesian coordinates of all the optimized geometries from density functional theory (DFT) calculations are provided as Supplementary Materials, together with computed Hg-M and Hg-Y bond lengths and M-Hg-Y angles (Table S1). The stationary points obtained for $[Cr(HgCl)(\eta^5\text{-}C_5H_5)(CO)_3]$ and $[Co(HgCl)(\eta^5\text{-}C_5H_5)(CO)_2]^+$ are depicted as examples in Figure 14. The M-Hg bond lengths show a slight increase (0.02 Å or less) moving from Y = Cl to Y = I. The M-Hg-Y angles are between 175.0 and 177.5° for Group 6 derivatives and between 177.3 and 179.7° for Group 9 complexes. The lower linearity of the {M-Hg-Y} fragments experimentally observed in a number of cases appears to be attributable to intermolecular interactions such as Hg···Y contacts.

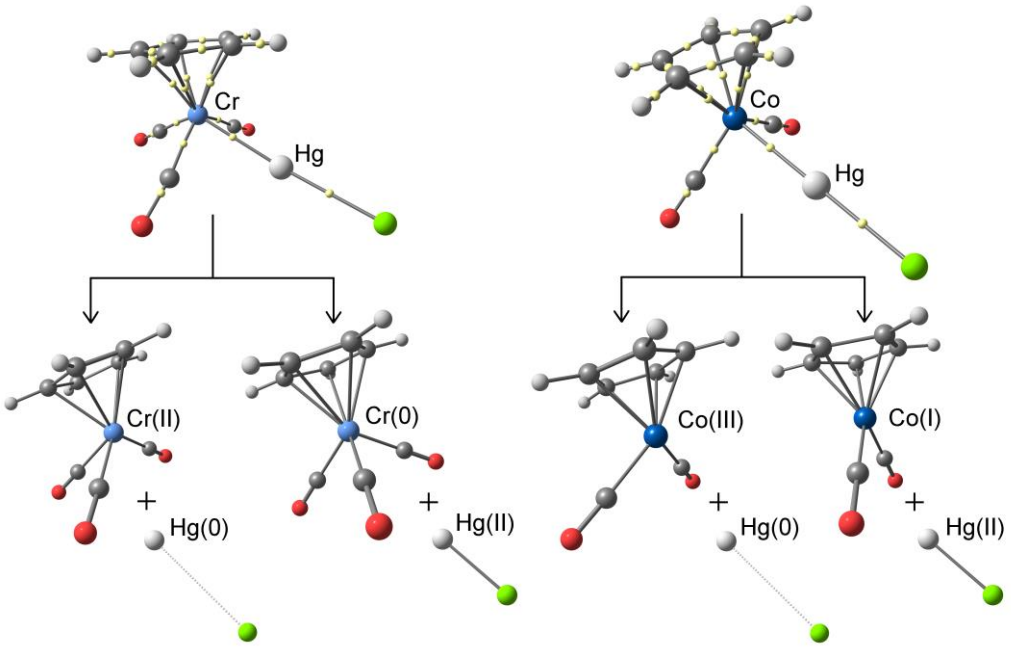

Figure 14. DFT-optimized structures of $[Cr(HgCl)(\eta^5\text{-}C_5H_5)(CO)_3]$ and $[Co(HgCl)(\eta^5\text{-}C_5H_5)(CO)_2]^+$ and products of the heterolytic Hg-M dissociation reactions [C-PCM/r^{2}SCAN-3c calculations]. Color map: Hg, light grey; Co, blue; Cr, light blue; Cl, light green; O, red; C, grey; H, white. (3, −1) BCPs represented as small light yellow spheres. Selected computed bond lengths (Å) and angles (°): $[Cr(HgCl)(\eta^5\text{-}C_5H_5)(CO)_3]$, Hg-Cr 2.611, Hg-Cl 2.431, Hg-Cr-Cl 175.0; $[Co(HgCl)(\eta^5\text{-}C_5H_5)(CO)_2]^+$, Hg-Co 2.495, Co-Cl 2.378, Hg-Co-Cl 179.6. Computed values at Hg-M (3, −1) BCPs [a.u.]: M = Cr, ρ 0.054, V −0.048, E −0.015, ∇^2 ρ 0.074; M = Co, ρ 0.065, V −0.059, E −0.017, ∇^2ρ 0.102.

The Gibbs energy variation for the heterolysis reactions $[M(HgY)(\eta^5\text{-}C_5H_5)(CO)_x]^{n+} \rightarrow [M(\eta^5\text{-}C_5H_5)(CO)_x]^{(n+1)+} + [HgY]^-$ and $[M(HgY)(\eta^5\text{-}C_5H_5)(CO)_x]^{n+} \rightarrow [M(\eta^5\text{-}C_5H_5)(CO)_x]^{(n-1)+} + [HgY]^+$ [n = 0, x = 3, M = Group 6; n = 1, x = 2, M = Group 9] were calculated by means of DFT calculations in the presence of acetone as continuous medium (Table 1). The first dissociation affords $[HgY]^-$ anions that behave as Lewis bases toward divalent Group 6 and trivalent Group 9 metal centers. Mercury can be considered as Hg(0). On the other hand, the $[HgY]^+$ cations generated by the second pathway contain divalent mercury, and they interact with transition metal fragments that behave as Lewis bases thanks to their electron-rich metal centers.

The heterolysis with the lowest Gibbs energy variation should suggest the most reasonable formal oxidation states for mercury and transition metals in the complexes. As observable in Table 1, the Group 6 and Group 9 derivatives here considered have opposite behavior. The dissociation of $[HgY]^-$ from $[M(HgY)(\eta^5\text{-}C_5H_5)(CO)_3]$ [M = Cr, Mo, W] is the most favorable path, so the compounds appear better described as M(II) complexes where the coordination sites are occupied by three carbonyls, a cyclopentadienyl ligand and $[HgY]^-$. It is worth noting the low influence of the nature of both M and Y on the ΔG values, comprised between 51.1 and 55.4 kcal mol^{-1}. The scarce energy variations on changing Y are in part attributable to the weak interactions between mercury and halides in $[HgY]^-$. On the contrary, the heterolytic dissociations of the Hg-M bonds in $[M(HgY)(\eta^5\text{-}C_5H_5)(CO)_2]^+$ [M = Co, Rh, Ir] should preferentially afford the $[HgY]^+$ cations. Therefore, in the Group 9 derivatives, the mercury center is probably best described as Hg(II), behaving as Lewis acid towards electron-rich M(I) complexes. As in the previous cases, the choice of M scarcely affects the Gibbs energy variations. On the other hand, the dissociation requires less energy on increasing the atomic number of the halide, probably because of the increased stability of $[HgY]^+$ with softer halides.

Table 1. Computed Gibbs energy variations [kcal mol^{-1}; C-PCM/r^{2}SCAN-3c calculations] for the heterolysis of the M-Hg bonds in selected complexes. C-PCM/r^{2}SCAN-3c, acetone as continuous medium.

Complex	$[M(HgY)L_n]^{n+} \rightarrow [ML_n]^{(n-1)+} + [HgY]^+$	$[M(HgY)L_n]^{n+} \rightarrow [ML_n]^{(n+1)+} + [HgY]^-$
$[Cr(HgCl)(\eta^5\text{-}C_5H_5)(CO)_3]$	76.8	52.5
$[Cr(HgBr)(\eta^5\text{-}C_5H_5)(CO)_3]$	73.2	51.1
$[Cr(HgI)(\eta^5\text{-}C_5H_5)(CO)_3]$	67.2	51.1
$[Mo(HgCl)(\eta^5\text{-}C_5H_5)(CO)_3]$	78.6	53.1
$[Mo(HgBr)(\eta^5\text{-}C_5H_5)(CO)_3]$	74.8	51.6
$[Mo(HgI)(\eta^5\text{-}C_5H_5)(CO)_3]$	68.6	51.3
$[W(HgCl)(\eta^5\text{-}C_5H_5)(CO)_3]$	80.1	55.4
$[W(HgBr)(\eta^5\text{-}C_5H_5)(CO)_3]$	76.2	53.7
$[W(HgI)(\eta^5\text{-}C_5H_5)(CO)_3]$	69.9	53.4
$[Co(HgCl)(\eta^5\text{-}C_5H_5)(CO)_2]^+$	51.1	87.1
$[Co(HgBr)(\eta^5\text{-}C_5H_5)(CO)_2]^+$	47.8	85.9
$[Co(HgI)(\eta^5\text{-}C_5H_5)(CO)_2]^+$	42.7	86.7
$[Rh(HgCl)(\eta^5\text{-}C_5H_5)(CO)_2]^+$	51.9	81.2
$[Rh(HgBr)(\eta^5\text{-}C_5H_5)(CO)_2]^+$	48.5	80.1
$[Rh(HgI)(\eta^5\text{-}C_5H_5)(CO)_2]^+$	43.3	80.8
$[Ir(HgCl)(\eta^5\text{-}C_5H_5)(CO)_2]^+$	55.9	87.6
$[Ir(HgBr)(\eta^5\text{-}C_5H_5)(CO)_2]^+$	52.3	86.2
$[Ir(HgI)(\eta^5\text{-}C_5H_5)(CO)_2]^+$	46.8	86.7

The outcome of the charge decomposition analysis on [Cr(HgCl)(η^5-C_5H_5)$(CO)_3$], partitioned as [Cr(η^5-C_5H_5)$(CO)_3$]$^+$ and [HgCl]$^-$, was {HgCl}→{Cr(η^5-C_5H_5)$(CO)_3$} donation of 0.222 electrons, while the opposite process resulted limited to 0.083 electrons. The same analysis on [Co(HgCl)(η^5-C_5H_5)$(CO)_2$]$^+$, partitioned as [Co(η^5-C_5H_5)$(CO)_2$] and [HgCl]$^+$, afforded {Co(η^5-C_5H_5)$(CO)_3$}→{HgCl} donation of 0.258 electrons, and only 0.021 electrons resulted back-donated. Roughly comparable values were obtained on changing the halide and the metal center, as reported in Table S2.

The Atoms-in-Molecules (AIM) analysis on [Cr(HgCl)(η^5-C_5H_5)$(CO)_3$] and [Co(HgCl)(η^5-C_5H_5)$(CO)_2$]$^+$ revealed the presence of Hg-M (3, −1) bond critical points (BCPs) characterized by quite high values of electron density (ρ) and absolute values of potential energy density (V). The energy density (E) values are negative and the Laplacian of electron density ($\nabla^2\rho$) is positive, in line with Bianchi's definition of metal–metal bond [154]. Selected data for the two compounds are collected in the caption of Figure 14. The occupied molecular orbitals mainly responsible for the Hg-M σ-overlaps are shown in Figure 15.

The AIM data for the other compounds, summarized in Table S3, indicate scarce influence of the nature of the halide on the ρ and V values at Hg-M (3, −1) BCP. For what concerns the Hg-Cl (3, −1) BCPs, the ρ and V values highlight a stronger bond in the cobalt derivative [ρ = 0.084 a.u., V = −0.094 a.u.) respect to the chromium complex [ρ = 0.075 a.u., V = −0.082 a.u.]. Such a result appears in line with the greater Lewis acid behavior proposed for the mercury center in [Co(HgCl)(η^5-C_5H_5)$(CO)_2$]$^+$ respect to [Cr(HgCl)(η^5-C_5H_5)$(CO)_3$]. The AIM data at Hg-Y (3, −1) BCP remain roughly constant by replacing the metal center with heavier congeners, as observable in Table S3. The different strength of the Hg-Cl bonds was confirmed by the computed Mayer bond orders [155], equal to 0.670 in [Co(HgCl)(η^5-C_5H_5)$(CO)_2$]$^+$ and 0.580 in [Cr(HgCl)(η^5-C_5H_5)$(CO)_3$]. Despite all the differences, the Hg-M Mayer bond order values in [Cr(HgCl)(η^5-C_5H_5)$(CO)_3$] and [Co(HgCl)(η^5-C_5H_5)$(CO)_2$]$^+$ are strictly comparable, respectively equal to 0.650 and 0.646.

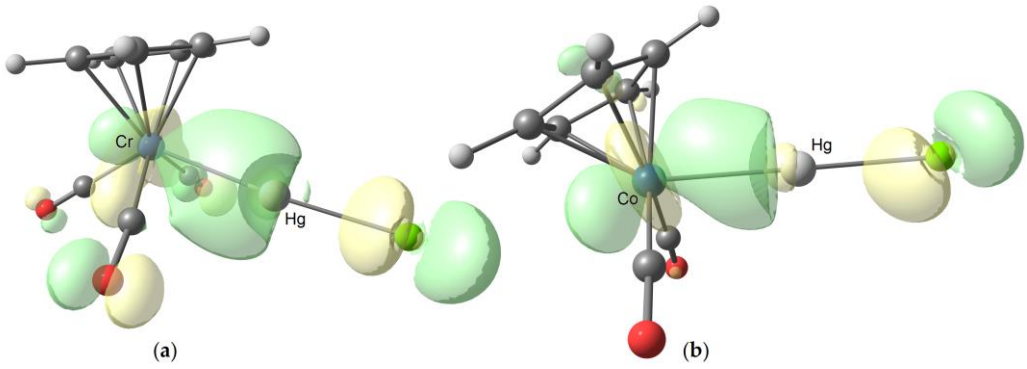

Figure 15. DFT-optimized structures of (**a**) [Cr(HgCl)(η^5-C_5H_5)$(CO)_3$] and (**b**) [Co(HgCl)(η^5-C_5H_5)$(CO)_2$]$^+$ with plots of the occupied molecular orbitals mainly responsible for the Hg-M σ-overlaps. Color map: Hg, light grey; Co, blue; Cr, light blue; Cl, light green; O, red; C, grey; H, white. Surfaces in yellow and green tones, isovalue = 0.04 a.u.

5. Computational Methods

The geometry optimizations were carried out with the r^{2}SCAN-3c method [156], based on the *meta*-GGA r^{2}SCAN functional [157] combined with a tailor-made triple-ζ Gaussian atomic orbital basis set, with relativistic effective core potentials for mercury and the heavier atoms [158,159]. The method also includes refitted D4 and geometrical counter-poise corrections for London dispersion and basis set superposition error [160,161]. The C-PCM implicit solvation model was added, considering acetone as continuous medium [162]. IR simulations were carried out using the harmonic approximation, from which zero-point vibrational energies and thermal corrections (T = 298.15 K) were obtained. Calculations

were carried out using ORCA version 5.0.3 [163,164] and the output files were analyzed with Multiwfn version 3.8 [165].

6. Conclusions

The chemistry of heteropolymetallic transition metal–mercury compounds is complex and fascinating, and the examples provided in this review do not complete the portrait of possibilities offered by the presence of M-Hg bonds. As an example, iron–mercury clusters with high nuclearities and intriguing structures were isolated and characterized by Fenske and co-workers by reacting $[Fe(HgY)_2(CO)_4]$ derivatives with phosphines and related species [166].

The present review is focused on mercury monohalides, whose modes of interaction with transition metal fragments are qualitatively comparable with those of the hydrogen atom thanks to the isolobal analogy. The {HgY} fragment, however, offers peculiar possibilities, such as the displacement of the halide and the presence of intra- and intermolecular mercurophilic and mercury–halide interactions. Mercury is also of interest because of the high atomic number and the consequent relativistic effects induced in transition metal compounds. Despite the well-known toxicity of mercury, which limits the use of its derivatives in synthetic chemistry, mercury monohalides can be considered as unusual ligands able to promote uncommon chemical and physical features in organometallic compounds, of potential interest in the fields of catalysis and functional materials.

Supplementary Materials: The following supporting information can be downloaded at: https://www.mdpi.com/article/10.3390/molecules30010145/s1, Table S1: Selected computed bond lengths and angles for $[M(HgY)(\eta^5\text{-}C_5H_5)(CO)_3]$ [M = Cr, Mo, W; Y = Cl, Br, I] and $[M(HgY)(\eta^5\text{-}C_5H_5)(CO)_2]^+$ [M = Cr, Mo, W; Y = Cl, Br, I]; Table S2: Output of the charge decomposition analysis on $[M(HgY)(\eta^5\text{-}C_5H_5)(CO)_3]$ [M = Cr, Mo, W; Y = Cl, Br, I], partitioned as $[M(\eta^5\text{-}C_5H_5)(CO)_3]^+$ and $[HgY]^-$, and on $[M(HgY)(\eta^5\text{-}C_5H_5)(CO)_2]^+$ [M = Cr, Mo, W; Y = Cl, Br, I], partitioned as $[M(\eta^5\text{-}C_5H_5)(CO)_2]$ and $[HgY]^+$; Table S3: AIM data for the Hg-M and Hg-Y (3, −1) BCPs in $[M(HgY)(\eta^5\text{-}C_5H_5)(CO)_3]$ [M = Cr, Mo, W; Y = Cl, Br, I] and $[M(HgY)(\eta^5\text{-}C_5H_5)(CO)_2]^+$ [M = Cr, Mo, W; Y = Cl, Br, I]; List S1: Cartesian coordinates of the DFT-optimized structures.

Author Contributions: Conceptualization, M.B. (Marco Bortoluzzi); methodology, M.B. (Matteo Busato), J.C. and M.B. (Marco Bortoluzzi); validation, M.B. (Matteo Busato), J.C., D.P. and M.B. (Marco Bortoluzzi); formal analysis, M.B. (Matteo Busato), J.C. and M.B. (Marco Bortoluzzi); investigation, M.B. (Matteo Busato), J.C., D.P. and M.B. (Marco Bortoluzzi); resources, J.C. and M.B. (Marco Bortoluzzi); data curation, M.B. (Matteo Busato), J.C., D.P. and M.B. (Marco Bortoluzzi); writing—original draft preparation, M.B. (Matteo Busato), J.C., D.P. and M.B. (Marco Bortoluzzi); writing—review and editing, M.B. (Matteo Busato), J.C., D.P. and M.B. (Marco Bortoluzzi); visualization, J.C.; supervision, M.B. (Marco Bortoluzzi); project administration, M.B. (Marco Bortoluzzi); funding acquisition, M.B. (Marco Bortoluzzi) All authors have read and agreed to the published version of the manuscript.

Funding: This work is part of the "Network 4 Energy Sustainable Transition-NEST" project (MIUR project code PE000021, Concession Degree No. 1561 of 11 October 2022), in the framework of the NextGenerationEu PNRR plan (CUP C93C22005230007).

Institutional Review Board Statement: Not applicable.

Informed Consent Statement: Not applicable.

Data Availability Statement: Data are contained within the article and Supplementary Materials.

Acknowledgments: CINECA (Bologna, Italy) is gratefully acknowledged for computational resources and support.

Conflicts of Interest: The authors declare no conflicts of interest. The funders had no role in the design of the study; in the collection, analyses, or interpretation of data; in the writing of the manuscript; or in the decision to publish the results.

References

1. Lewis, J. Metal-metal interaction in transition metal complexes. *Pure Appl. Chem.* **1965**, *10*, 11–36. [CrossRef]
2. Burlitch, J.M. Compounds with Bonds between Transition Metals and either Mercury, Cadmium, Zinc or Magnesium. In *Comprehensive Organometallic Chemistry*; Wilkinson, G., Stone, F.G.A., Abel, E.W., Eds.; Pergamon Press: Oxford, UK, 1982; Volume 6, pp. 983–1041. [CrossRef]
3. Dean, P.A.W. Mercury as a Ligand. In *Comprehensive Coordination Chemistry*; Wilkinson, G., Gillard, R.D., McCleverty, J.A., Eds.; Pergamon Press: Oxford, UK, 1987; Volume 2, pp. 1–6.
4. Gade, L.H. Mercury, a Structural Building Block and Source of Localized Reactivity in Extended Metal-Metal Bonded Systems. *Angew. Chem. Int. Ed.* **1993**, *32*, 24–40. [CrossRef]
5. Rosenberg, E.; Hardcastle, K.I. Cluster Complexes with Bonds Between Transition Elements and Zinc, Cadmium, and Mercury. In *Comprehensive Organometallic Chemistry II*; Abel, E.W., Gordon, F., Stone, A., Wilkinson, G., Eds.; Elsevier: Amsterdam, The Netherlands, 1995; Volume 10, pp. 323–350. [CrossRef]
6. Ara, I.; Forniés, J.; Gabilondo, L.; Usón, M.A. New Pt-Hg clusters with pentachlorophenyl groups. *Inorg. Chim. Acta* **2003**, *347*, 155–160. [CrossRef]
7. Wright, C.A.; Brand, U.; Shapley, J.R. Synthesis and Characterization of the Dimercury(I)-Linked Compound $[PPN]_4[(Re_7C(CO)_{21}Hg)_2]$. Oxidative Cleavage of the Mercury-Mercury Bond Leading to Carbidoheptarhenate Complexes of Mercury(II), Including $[PPN][Re_7C(CO)_{21}Hg(S{=}C(NMe_2)_2)]$. *Inorg. Chem.* **2021**, *40*, 4091–4896. [CrossRef]
8. Catalano, V.J.; Malwitz, M.A. Pd(0) and Pt(0) Metallocryptands Encapsulating a Spinning Mercurous Dimer. *Inorg. Chem.* **2002**, *41*, 6553–6559. [CrossRef]
9. Tanase, T.; Goto, E.; Takenaka, H.; Horiuchi, T.; Yamamoto, Y.; Kuwabara, J.; Osakada, K. Cage-Type Hexanuclear Platinum(0) Clusters with Diphosphine and Isocyanide Ligands Encapsulating Two Mercury(0) Atoms. *Organometallics* **2005**, *24*, 234–244. [CrossRef]
10. Weil, M. Single Crystal Growth and Crystal Structure of Anhydrous Mercury(I) Nitrate, $Hg_2(NO_3)_2$. *Z. Anorg. Allg. Chem.* **2003**, *629*, 1547–1552. [CrossRef]
11. Kreye, M.; Freytag, M.; Jones, P.G.; Williard, P.G.; Bernskoetter, W.H.; Walter, M.D. Homolytic H_2 cleavage by a mercury-bridged Ni(I) pincer complex $[\{(PNP)Ni\}_2\{\mu\text{-}Hg\}]$. *Chem. Commun.* **2015**, *51*, 2946–2949. [CrossRef]
12. Song, L.-C.; Yang, H.; Dong, Q.; Hu, Q.-M. Unexpected metal-metal bond formation in the M-Hg-M (M = Cr, Mo, W) structural unit. Synthesis and characterization of $[\eta^5\text{-}RC_5H_4(CO)_3M]_2Hg$ complexes (R = H, M = W; R= CH_3CO, M = Cr, Mo, W). *J. Organomet. Chem.* **1991**, *414*, 137–143. [CrossRef]
13. Johnson, B.F.G.; Kwik, W.-L.; Lewis, J.; Raithby, P.R.; Saharan, V.P. Synthesis of mercury-linked ruthenium clusters: The X-ray structure of the new cluster dianion $[\{Ru_6C(CO)_{16}\}_2Hg]^{2-}$ and the cluster $[\{Ru_5C(CO)_{14}(\mu\text{-}Cl)\}_2Hg_2Cl_2]$. *J. Chem. Soc. Dalton Trans.* **1991**, 1037–1042. [CrossRef]
14. Andreu, P.L.; Cabeza, J.A.; Llamazares, A.; Riera, V.; Bois, B.; Jeannin, Y. Mercury—Ruthenium mixed-metal carbonyl clusters containing 2-amido-6-methylpyridine (ampy) as a μ_3,η^2-ligand. Crystal structures of $[Ru_6(\mu_4\text{-}Hg)(\mu_3\text{-}ampy)_2(CO)_{18}]\cdot 2C_4H_8O$ and $[Ru_3(\mu\text{-}HgBr)(\mu_3\text{-}ampy)(CO)_9]$. *J. Organomet. Chem.* **1991**, *420*, 431–442. [CrossRef]
15. Cesari, C.; Bortoluzzi, M.; Femoni, C.; Iapalucci, M.C.; Zacchini, S. Mercurophilic interactions in heterometallic Ru-Hg carbonyl clusters. *Inorg. Chim. Acta* **2023**, *545*, 121281. [CrossRef]
16. Cheung, W.-M.; Chong, M.-C.; Sung, H.H.-Y.; Cheng, S.-C.; Williams, I.D.; Ko, C.-C.; Leung, W.H. Synthesis, structure and reactivity of iridium complexes containing a bis-cyclometalated tridentate CˆNˆC ligand. *Dalton Trans.* **2021**, *50*, 8512–8523. [CrossRef] [PubMed]
17. Reina, R.; Riba, O.; Rossell, O.; Seco, M.; de Montauzon, D.; Font-Bardia, M.; Solans, X. Cobalt/Mercury Carbide Clusters Based on Trigonal-Prismatic or Octahedral Co_6C Skeletons—X-ray Crystal Structure of $(NEt_4)_2[Co_6C(CO)_{12}\{HgW(CO)_3Cp\}_2]$. *Eur. J. Inorg. Chem.* **2001**, *2001*, 1243–1249. [CrossRef]
18. Haupt, H.-J.; Merla, A.; Flörke, U. Heterometallische Clusterkomplexe der Typen $Re_2(\mu\text{-}PR_2)(CO)_8(HgY)$ und $ReMo(\mu\text{-}PR_2)(\eta^5\text{-}C_5H_5)(CO)_6(HgY)$ (R = Ph, Cy; Y = Cl, $W(\eta^5\text{-}C_5H_5)(CO)_3$). *Z. Anorg. Allg. Chem.* **1994**, *620*, 999–1005. [CrossRef]
19. Rupf, S.M.; Pan, S.; Moshtaha, A.L.; Frenking, G.; Malischewski, M. Structural Characterization and Bonding Analysis of $[Hg\{Fe(CO)_5\}_2]^{2+}$ $[SbF_6]^-{}_2$. *J. Am. Chem. Soc.* **2023**, *145*, 15353–15359. [CrossRef]
20. Alvarez, S.; Ferrer, M.; Reina, R.; Rossell, O.; Seco, M. Anionic trimetallic compounds containing Fe-E-M skeletons (E = Zn, Cd, Hg; M = Fe, MO, W). Crystal structure of $[NPPh_3)_2]_2[(OC)_4Fe\text{-}Hg\text{-}Fe(CO)_4]$. *J. Organomet. Chem.* **1989**, *377*, 291–303. [CrossRef]

21. Sosinsky, B.A.; Shong, R.G.; Fitzgerald, B.J.; Norem, N.; O'Rourke, C. Reduction of the Group IIB tetracarbonylferrates in Lewis bases. Synthesis, characterization, and structural features of the $(Na\{THF\}_2)^+_2[M'(Fe(CO)_4)_2]^{2-}$ (M′ = Zn, Cd, and Hg) series. *Inorg. Chem.* **1983**, *22*, 3124–3129. [CrossRef]
22. Schmidbaur, H.; Schier, A. Mercurophilic Interactions. *Organometallics* **2015**, *34*, 2048–2066. [CrossRef]
23. Echeverría, J.; Cirera, J.; Alvarez, S. Mercurophilic interactions: A theoretical study on the importance of ligands. *Phys. Chem. Chem. Phys.* **2017**, *19*, 11645–11654. [CrossRef]
24. Pyykkö, P. Strong Closed-Shell Interactions in Inorganic Chemistry. *Chem. Rev.* **1997**, *97*, 597–636. [CrossRef] [PubMed]
25. Vreshch, V.; Shen, W.; Nohra, B.; Yip, S.-K.; Yam, V.W.-W.; Lescop, C.; Réau, R. Aurophilicity versus Mercurophilicity: Impact of d^{10}–d^{10} Metallophilic Interactions on the Structure of Metal-Rich Supramolecular Assemblies. *Chem. Eur. J.* **2012**, *18*, 466–477. [CrossRef] [PubMed]
26. Gade, L.H.; Johnson, B.F.G.; Lewis, J.; Conole, G.; McPartlin, M. Redox–chemical core manipulation of $[Os_{18}Hg_3C_2(CO)_{42}]^{2-}$; synthesis and crystal structure of the cluster $[Os_{18}Hg_2C_2(CO)_{42}]^{4-}$. *J. Chem. Soc. Dalton Trans.* **1992**, 3249–3254. [CrossRef]
27. Gade, L.H.; Johnson, B.F.G.; Lewis, J.; McPartlin, M.; Kotch, T.; Lees, A.J. Photochemical core manipulation in high-nuclearity osmium-mercury clusters. *J. Am. Chem. Soc.* **1991**, *113*, 8698–8704. [CrossRef]
28. Chiaradonna, G.; Ingrosso, G.; Marchetti, F. $[\{Ir(\eta^5\text{-}C_5Me_5)CO)\}_6Hg_8][CF_3CO_2]_6$, a Mixed-Metal Cluster with an Ir_6Hg_6 Twelve-Membered Ring and Additional Hg Centers and Metal-Metal Bonds. *Angew. Chem. Int. Ed.* **2000**, *39*, 3872–3873. [CrossRef]
29. Levason, W.; McAuliffe, C.A. The Coordination Chemistry of Mercury. In *The Chemistry of Mercury. Aspects of Inorganic Chemistry*; McAuliffe, C.A., Ed.; Palgrave Macmillan: London, UK, 1977; pp. 47–135.
30. Ali Morsali, A.; Masoomi, M.Y. Structures and properties of mercury(II) coordination polymers. *Coord. Chem. Rev.* **2009**, *253*, 1882–1905. [CrossRef]
31. Melnik, M. Isomers in the chemistry of mercury coordination compounds. *Cent. Eur. J. Chem.* **2010**, *8*, 469–485. [CrossRef]
32. Samie, A.; Salimi, A.; Garrison, J.C. Coordination chemistry of mercury(II) halide complexes: A combined experimental, theoretical and (ICSD & CSD) database study on the relationship between inorganic and organic units. *Dalton Trans.* **2020**, *49*, 11859–11877. [CrossRef]
33. Beletskaya, I.P. In My Element: Mercury. *Chem. Eur. J.* **2019**, *25*, 7408–7409. [CrossRef]
34. Raju, S.; Singh, H.B.; Butcher, R.J. Metallophilic interactions: Observations of the shortest metallophilic interactions between closed shell ($d^{10}\cdots d^{10}$, $d^{10}\cdots d^8$, $d^8\cdots d^8$) metal ions [M···M′ M = Hg(II) and Pd(II) and M′ = Cu(I), Ag(I), Au(I), and Pd(II)]. *Dalton Trans.* **2020**, *49*, 9099–9117. [CrossRef]
35. Tagne Kuate, A.C.; Lalancette, R.A.; Bockfeld, D.; Tamm, M.; Jäkle, F. Palladium(0) complexes of diferrocenylmercury diphosphines: Synthesis, X-ray structure analyses, catalytic isomerization, and C–Cl bond activation. *Dalton Trans.* **2021**, *50*, 4512–4518. [CrossRef] [PubMed]
36. Tagne Kuate, A.C.; Lalancette, R.A.; Bannenberg, T.; Tamm, M.; Jäkle, F. Diferrocenylmercury diphosphine diastereomers with unique geometries: Trans-chelation at Pd(II) with short Hg(II)···Pd(II) contacts. *Dalton Trans.* **2019**, *48*, 13430–13439. [CrossRef] [PubMed]
37. López-de-Luzuriaga, J.M.; Monge, M.; Olmos, M.E.; Pascual, D. Study of the Nature of Closed-Shell $Hg^{II}\cdots M^{I}$ (M = Cu, Ag, Au) Interactions. *Organometallics* **2015**, *34*, 3029–3038. [CrossRef]
38. Martin, A.; Bennett, M.A.; Contel, M.; Hockless, D.C.R.; Welling, L.L.; Willis, A.C. Bis{(2-diphenylphosphino)phenyl}mercury: A P-Donor Ligand and Precursor to Mixed Metal−Mercury (d^8-d^{10}) Cyclometalated Complexes Containing 2-$C_6H_4PPh_2$. *Inorg. Chem.* **2002**, *41*, 844–855. [CrossRef]
39. Tagne Kuate, A.C.; Lalancette, R.A.; Bannenberg, T.; Jäkle, F. Diferrocenylmercury-Bridged Diphosphine: A Chiral, Ambiphilic, and Redox-Active Bidentate Ligand. *Angew. Chem. Int. Ed.* **2018**, *57*, 6552–6557. [CrossRef]
40. López-de-Luzuriaga, J.M.; Monge, M.; Olmos, M.E.; Pascual, D. Experimental and Theoretical Comparison of the Metallophilicity between d^{10}–d^{10} Au^{I}–Hg^{II} and d^8–d^{10} Au^{III}–Hg^{II} Interactions. *Inorg. Chem.* **2014**, *53*, 1275–1277. [CrossRef]
41. Patel, U.; Sharma, S.; Singh, H.B.; Dey, S.; Jain, V.K.; Wolmershäuser, G.; Butcher, R.J. Intermetallic Bonds in Metallophilic Mercuraazametallamacrocycles of Synthetic Design. *Organometallics* **2010**, *29*, 4265–4275. [CrossRef]
42. Patel, U.; Singh, H.B.; Wolmershäuser, G. Synthesis of a Metallophilic Metallamacrocycle: A $Hg^{II}\cdots Cu^{I}\cdots Hg^{II}\cdots Hg^{II}\cdots Cu^{I}\cdots Hg^{II}$ Interaction. *Angew. Chem. Int. Ed.* **2005**, *44*, 1715–1717. [CrossRef]
43. López-de-Luzuriaga, J.M.; Monge, M.; Olmos, M.E.; Pascual, D.; Lasanta, T. Amalgamating at the molecular level. A study of the strong closed-shell Au(I)···Hg(II) interaction. *Chem. Commun.* **2011**, *47*, 6795–6797. [CrossRef]
44. Lasanta, T.; López-de-Luzuriaga, J.M.; Monge, M.; Olmos, M.E.; Pascual, D. Synthesis of the molecular amalgam $[\{AuHg_2(o\text{-}C_6F_4)_3\}\{Hg_3(o\text{-}C_6F_4)_3\}]^-$: A rare example of a heterometallic homoleptic metallacycle. *Dalton Trans.* **2016**, *45*, 6334–6338. [CrossRef]
45. Kim, M.; Taylor, T.J.; Gabbaï, F.P. Hg(II)···Pd(II) Metallophilic Interactions. *J. Am. Chem. Soc.* **2008**, *130*, 6332–6333. [CrossRef] [PubMed]

46. Simon, M.; Jönk, P.; Wühl-Couturier, G.; Halbach, S. Mercury, Mercury Alloys, and Mercury Compounds. In *Ullmann's Encyclopedia of Industrial Chemistry*; Wiley-VCH: Weinheim, Germany, 2012; Volume 22, pp. 578–580. [CrossRef]
47. Ginzburg, A.G.; Aleksandrov, G.G.; Struchkov, Y.T.; Setkina, V.N.; Kursanov, D.N. Basicity of transiton metal carbonyl complexes: XIII. Reactions of the π-cyclopentadienyl complexes of molybdenum and tungsten with aprotic acids. *J. Organomet. Chem.* **1980**, *199*, 229–242. [CrossRef]
48. Edelmann, F.; Behrens, P.; Behrens, S.; Behrens, U. Übergangsmetall-fulven-komplexe: XXVII. Basische fulven-komplexe. *J. Organomet. Chem.* **1986**, *309*, 109–116. [CrossRef]
49. Pardo, M.P.; Cano, M. Reactions of tricarbonylpyridine complexes (NN)(py)M(CO)$_3$ (M = Mo, W.; NN = 2,2′-bipyridine, 1,10-phenanthroline) with mercuric derivatives HgX_2 (X = Cl, CN, SCN). *J. Organomet. Chem.* **1984**, *270*, 311–318. [CrossRef]
50. Touchard, D.; Lelay, C.; Fillaut, J.-L.; Dixneuf, P.H. A Novel Roue to Thiocarbonyl-Metal Complexes via Electron Transfer to (η^2-CS_2R)-Metal Cations. *J. Chem. Soc. Chem. Commun.* **1986**, 37–38. [CrossRef]
51. Adams, D.M.; Cook, D.J.; Kemmitt, R.D.W. Reactions of mercuric halides with some substituted iron carbonyls; infrared spectra of the products and related adducts. *J. Chem. Soc. A* **1968**, 1067–1072. [CrossRef]
52. Cook, D.J.; Dawes, J.L.; Kemmitt, R.D.W. Some mercury halide–cobalt and –rhodium compounds. *J. Chem. Soc. A* **1967**, 1547–1551. [CrossRef]
53. Lewis, J.; Wild, S.B. Chemistry of polynuclear compounds. Part IV. Some amine-substituted mercury halide–iron carbonyl compounds. *J. Chem. Soc. A* **1966**, 69–72. [CrossRef]
54. Lobo, M.A.; Perpiñan, M.F.; Pardo, M.P.; Cano, M. Reactions of the carbonyl complexes M(CO)$_3$(L)$_3$ (L = py, M = Mo, W.; L = NH_3, M = Mo) and M(CO)$_4$(2-Mepy)$_2$ (M = Mo, W) with HgX_2 (X = Cl, CN, SCN). *J. Organomet. Chem.* **1983**, *254*, 325–332. [CrossRef]
55. Graddon, D.P.; Gregor, I.K.; Siddiqi, I.A. Stability and bond strength in adducts of mercury(II) halides with transition metal carbonyl derivatives. *J. Organomet. Chem.* **1975**, *102*, 321–326. [CrossRef]
56. Coco, S.; Espinet, P.; Mayor, F.; Solans, X. Insertion of mercury into iron–halogen bonds. X-Ray structure of [(p-$MeC_6H_4NC)_5Fe\rightarrow HgI_2$]. *J. Chem. Soc. Dalton Trans.* **1991**, 2503–2509. [CrossRef]
57. Coco, S.; Mayor, F. Insertion of mercury into iron-iodine bonds leading to dinuclear (Fe-Hg) mixed isonitrile-phosphine complexes. *J. Organomet. Chem.* **1994**, *464*, 215–218. [CrossRef]
58. Ehara, K.; Kumagaya, K.; Yamamoto, Y.; Takahashi, K.; Yamazaki, H. Unusual reductive behaviour of a trans-NiI_2(RNC)$_2$ complex at mercury and platinum electrodes. *J. Organomet. Chem.* **1991**, *410*, C49–C53. [CrossRef]
59. Xu, X.; Fang, L.; Chen, Z.-X.; Yang, G.-C.; Sun, S.-L.; Su, Z.-M. Quantum chemistry studies on the Ru–M interactions and the ^{31}P NMR in [Ru(CO)$_3$(Ph_2Ppy)$_2$(MCl_2)] (M = Zn, Cd, Hg). *J. Organomet. Chem.* **2006**, *691*, 1927–1933. [CrossRef]
60. Nowell, I.N.; Russell, D.R. The crystal structure of the dicarbonylcyclopentadienylcobalt–mercuric chloride complex. *Chem. Commun.* **1967**, 817. [CrossRef]
61. Carter, S.J.; Foxman, B.M.; Stuhl, L.S. Direct synthesis of low-valent acyl isocyanide metal complexes. Preparation, structure and properties of (η^5-C_5H_5)Co(CNCOR)$_2$ complexes formed via reaction of (η^5-C_5H_5)Co(CO)$_2$ with acyl isocyanides. *Organometallics* **1986**, *5*, 1918–1920. [CrossRef]
62. Le Bozec, H.; Dixneuf, P.H.; Adams, R.D. Stabilization of a metal-carbene intermediate by formation of a metal-mercury(II) bond. Synthesis and x-ray structure of [cyclic] Cl_2HgFe(:C+SC(CO_2Me):C(CO_2Me)S)(CO)$_2$(PMe_2Ph)$_2$. *Organometallics* **1984**, *12*, 1919–1921. [CrossRef]
63. Khasnis, D.V.; Le Bozec, H.; Dixneuf, P.H.; Adams, R.D. Formation of donor-acceptor Fe(0)→Hg(II) bond for the stabilization of carbene-iron(0) complexes: Synthesis, characterization, and reactivity toward sulfur donor molecules and x-ray structure of $Cl_2HgFe(CO)_2(PMe_2Ph)_2(CS_2C_2(CO_2Me)_2)$. *Organometallics* **1986**, *5*, 1772–1777. [CrossRef]
64. Sharp, P.R. Synthesis and characterization of a platinum-mercury "A-frame" cluster. *Inorg. Chem.* **1986**, *25*, 4185–4189. [CrossRef]
65. Faraone, F.; Lo Schiavo, S.; Bruno, G.; Bombieri, G. Mercury(II) chloride bridging two rhodium atoms. Preparation and X-ray crystal structure of [Rh_2(η-C_5H_5)$_2$(μ-CO)(μ-$Ph_2PCH_2PPh_2$)(μ-$HgCl_2$)]. *J. Chem. Soc. Chem. Commun.* **1984**, 6–7. [CrossRef]
66. Luo, G.-G.; Huang, R.-B.; Sun, D.; Lin, L.-R.; Zheng, L.-S. Synthesis, X-ray structures, and photoluminescence of heterometal trinuclear Hg(II)–Pt(I) and tetranuclear Hg(II)–Pd(I) complexes. *Inorg. Chem. Commun.* **2008**, *11*, 1337–1340. [CrossRef]
67. Kuang, S.-M.; Zhang, Z.-Z.; Chinnakali, K.; Fun, H.-K.; Mak, T.C.W. Formation of donor–acceptor Fe(0)–Hg(II) bond in separation and stabilization of optically active iron(0) phosphine complexes. Absolute configuration of (+)-(R)-(CO)$_4$Fe(μ-EtPhPpy)$HgCl_2$. *Inorg. Chim. Acta* **1999**, *293*, 106–109. [CrossRef]
68. Zhang, Z.-Z.; Cheng, H.; Kuang, S.-M.; Zhou, Y.-Q.; Liu, Z.-X.; Zhang, J.-K.; Wang, H.-G. Coordination chemistry of organometallic polydentate ligands. Studies on the syntheses and properties of Fe-M binuclear complexes prepared from organometallic tridentate ligand trans-Fe(CO)$_3$(Ph_2Ppy)$_2$ (Ph_2Ppy = 2-(diphenylphosphino)pyridine). *J. Organomet. Chem.* **1996**, *516*, 1–10. [CrossRef]
69. Li, S.-L.; Zhang, Z.-Z.; Mak, T.C.W. The new organometallic polydentate ligand *trans*-bis(2-(diphenylphosphino) pyrimidine) tricarbonyliron(0) and its mono-, di- and tridentate coordination modes towards mercury(II) halide/pseudohalide. *J. Organomet. Chem.* **1997**, *536–537*, 73–86. [CrossRef]

70. Song, H.-B.; Wang, Q.-M.; Zhang, Z.-Z.; Mak, T.C.W. Synthesis and structural characterization of hetero-binuclear complexes containing a $Fe^0 \rightarrow M^{n+}$ bond bridged by a non-rigid P,N-phosphine ligand. *J. Organomet. Chem.* **2000**, *605*, 15–21. [CrossRef]
71. Song, H.-B.; Zhang, Z.-Z.; Mak, T.C.W. Hetero-binuclear complexes containing a $Ru^0 \rightarrow M^{n+}$ bond bridged by P,N-phosphine ligands: Convenient synthesis of tridentate organometallic trans-$Ru(CO)_3(L)_2$ (L = phosphine bearing an N-donor substituent) ligands. *New. J. Chem.* **2002**, *26*, 113–119. [CrossRef]
72. Van der Ploeg, A.F.M.J.; Van Koten, G.; Vrieze, K.; Spek, A.L.; Duisenberg, A.J.M. Crystal structure and molecular geometry of a square-pyramidal platinum(II) complex [{2,6-$(Me_2NCH_2)_2C_6H_3$}Pt(μ-{(p-tol)NC(H)N(i-Pr)})HgBrCl] containing a Pt^{II}-to-Hg^{II} donor bond. *Organometallics* **1982**, *1*, 1066–1070. [CrossRef]
73. Balch, A.L.; Catalano, V.J. Reactivity of complexes with weak metal-metal bonds. Reactions of Lewis acids with AuIr(CO)Cl(μ-$Ph_2PCH_2PPh_2)_2$](PF_6). *Inorg. Chem.* **1992**, *31*, 2730–2734. [CrossRef]
74. Cabeza, J.A.; Fernández-Colinas, J.M.; García-Granda, S.; Riera, V.; Van der Maelen, J.F. Selective insertion of mercury(II) halides into the ruthenium–mercury bonds of trinuclear Ru_2Hg clusters. *J. Chem. Soc. Chem. Commun.* **1991**, 168–170. [CrossRef]
75. Cabeza, J.A.; Fernandez-Colinas, J.M.; Garcia-Granda, S.; Riera, V.; Van der Maelen, J.F. Addition of mercury(II) electrophiles to $[Ru_2(C_{10}H_8N_2)(CO)_4(P^iPr_3)_2]$ and selective insertion versus addition in the reactions of mercury(II) electrophiles with trinuclear diruthenium mercury clusters. X-ray structures of $[Ru_2Hg(O_2CCF_3)_2(C_{10}H_8N_2)(CO)_4(P^iPr_3)_2]$ and $[Ru_2Hg_2Cl_4(C_{10}H_8N_2)(CO)_4(P^iPr_3)_2]\cdot CH_2Cl_2$ ($C_{10}H_{10}N_2$ = 1,8-diaminonaphthalene). *Inorg. Chem.* **1992**, *31*, 1233–1238. [CrossRef]
76. Falvello, L.R.; Forniés, J.; Martín, A.; Navarro, R.; Sicilia, V.; Villarroya, P. Reactivity of [M(C∧P)(S_2C-R)] (M = Pd, Pt; C∧P = CH_2-C_6H_4-P(o-tolyl)$_2$-κC,P.; R = NMe_2, OEt) toward HgX_2 (X = Br, I). X-ray Crystal Structures of [Pt{CH_2-C_6H_4P(o-tolyl)$_2$-κC,P}(S_2CNMe_2)HgI(μ-I)]$_2$ and [PdBr(S_2COEt){μ-P(o-tolyl)$_2$-C_6H_4-CH_2-}HgBr]·0.5$HgBr_2$·$C_2H_4Cl_2$. *Inorg. Chem.* **1997**, *36*, 6166–6171. [CrossRef]
77. Yamamoto, Y.; Ehara, K.; Takahashi, K.; Yamazaki, H. Four- and Five-Coordinated Nickel(II) Isocyanide Complexes and Donor–Acceptor Complexes Containing Nickel and Mercury. *Bull. Chem. Soc. Jpn.* **1991**, *64*, 3376–3383. [CrossRef]
78. Alvarez, B.; Alvarez, M.A.; Amor, I.; García, M.E.; Ruiz, M.A.; Suárez, J. Gold(I) and Related Heterometallic Derivatives of Dimolybdenum Complexes with Asymmetric Phosphinidene Bridges. *Inorg. Chem.* **2014**, *53*, 10325–10339. [CrossRef] [PubMed]
79. Kuang, S.-M.; Cheng, H.; Sun, L.-J.; Zhang, Z.-Z.; Zhou, Z.-Y.; Wu, B.-M.; Mak, T.C.W. Coordination chemistry of organometallic polydentate ligands. Syntheses of Fe-M complexes using $Fe(CO)_4(Ph_2Ppy$-P)[Ph_2Ppy = 2-(diphenylphosphino)pyridine] and trans-$Fe(PhPMepy)_2(CO)_3$ [PhPMepy = 2-(phenylmethylphosphino)pyridine] as a neutral bi- or tridentate ligand. *Polyhedron* **1996**, *15*, 3417–3426. [CrossRef]
80. Kirk, R.M.; Hill, A.F. Arsolyl-supported intermetallic dative bonding. *Chem. Sci.* **2022**, *13*, 6830–6835. [CrossRef]
81. Ciplys, A.M.; Geue, R.J.; Snow, M.R. Crystal structure of the dimeric 1:2 addition complex of tricarbonylmesitylenemolybdenum with mercury(II) chloride. *J. Chem. Soc. Dalton Trans.* **1976**, 35–37. [CrossRef]
82. Ara, I.; Falvello, L.R.; Forniés, J.; Sicilia, V.; Villarroya, P. Reactivity of [M(C∧P)(acac-O,O′)] [M = Pt, Pd; C∧P = CH_2-C_6H_4-P(o-tolyl)$_2$-κC,P; acac = 2,4-pentanedionato] toward HgX_2 (X = Br, I, CH_3COO, CF_3COO). New Polynuclear Complexes Containing Pt−Hg Bonds. Molecular Structures of [{Pt(C∧P)(acac-O,O′)-HgBr(μ-Br)}$_2$(μ-$HgBr_2$)], an Unprecedented Square-Planar Bromomercurate Complex, and [{Pt(C∧P)(μ-O_2CCH_3)$_2$Hg(μ^3-acac^{2-}-κC^3,O)Hg(O_2CCH_3-κO)}·$CHCl_3$]$_2$, the First Complex Containing Asymmetric Dimercurated Acetylacetone. *Organometallics* **2000**, *19*, 3091–3099. [CrossRef]
83. Nowell, I.W.; Russell, D.R. Structures of mercury(II) halide adducts with transition-metal Lewis bases. Part II. Crystal structure of the 1:3 complex between dicarbonyl-π-cyclopentadienylcobalt and mercury(II) chloride. *J. Chem. Soc. Dalton Trans.* **1972**, 2396–2399. [CrossRef]
84. Einstein, F.W.B.; Yan, X.; Zhang, X.; Sutton, D. Characterization of 1:1 heterobimetallic complexes of (η^5-C_5Me_5)$Ir(CO)_2$ with zinc, cadmium and mercury(II) chloride and the X-ray structure determination of the 1:2 mercury complex. *J. Organomet. Chem.* **1992**, *439*, 221–230. [CrossRef]
85. Mays, M.J.; Robb, J.D. Exchange reactions involving transition-metal–mercury bonds. *J. Chem. Soc. A* **1968**, 329–332. [CrossRef]
86. Van Rentergem, M.; Van der Kelen, G.P. IR spectra of organophosphine substituted derivatives of (halomercury)tetracarbonylcobalt. *J. Mol. Struct.* **1985**, *127*, 47–55. [CrossRef]
87. Cano, M.; Campo, J.A. Reactivity of the Mo-Sn bond. Reactions of [$MoSnPh_3(CO)_3$(η-C_5H_5)] with HgX_2 (X = Cl, $OCOCF_3$). *Polyhedron* **1991**, *10*, 133–134. [CrossRef]
88. Roberts, R.M.G. Reactivity of Metal-Metal Bonds: I. Cleavage of molybdenum-tin and tungsten-tin bonds and synthesis of novel organomercury derivatives. *J. Organomet. Chem.* **1972**, *40*, 359–366. [CrossRef]
89. Roberts, R.M.G. Reactivity of metal-metal bonds: II. Exchange reactions of trimethyltin derivatives of manganese and iron. *J. Organomet. Chem.* **1973**, *47*, 359–366. [CrossRef]
90. Chipperfield, J.R.; Hayter, A.C.; Webster, D.E. Reactivity of main-group–transition-metal bonds. Part 7. Kinetics of the reaction of mercury(II) halides with compounds containing tin–chromium, –molybdenum, –tungsten, –manganese, –rhenium, and –iron bonds. *J. Chem. Soc. Dalton Trans.* **1977**, 485–490. [CrossRef]

91. Kumar, R.; Manning, A.R.; Murray, P.T. The reactions of $[Fe_2(\eta\text{-}C_5H_5)_2(CO)_{4-n}(CNMe)_n]$ (n = 0–4) complexes with halogens and mercury(II) salts. *J. Organomet. Chem.* **1987**, *323*, 53–65. [CrossRef]
92. Cano, M.; Panizo, M.; Campo, J.A.; Gutiérrez-Puebla, E.; Monge, M.A.; Ruiz-Valero, C. Reactivity of carbonyl complexes containing Mo-Hg bonds; reaction of tin(II) halides with $[Mo(CO)_3(NN)(HgX)(X)]$ (NN = bpy, phen, dmp); crystal structure of $[Mo(CO)_3(dmp)(HgCl)(Cl)]$. *Polyhedron* **1994**, *13*, 1669–1676. [CrossRef]
93. Fard, M.A.; Behnia, A.; Puddephatt, R.J. Stereochemistry of oxidative addition reactions of cycloneophyl complexes of Platinum(II): A methylene insertion reaction from dichloromethane. *J. Organomet. Chem.* **2019**, *890*, 32–42. [CrossRef]
94. McCready, M.S.; Puddephatt, R.J. The Platinum Center is a Stronger Nucleophile than the Free Nitrogen Donors in a Dimethylplatinum Complex with a Dipyridylpyridazine Ligand. *Organometallics* **2015**, *34*, 2261–2270. [CrossRef]
95. Janzen, M.C.; Jennings, M.C.; Puddephatt, R.J. Mechanism of Oxidative Addition of Mercury(II) Compounds to Platinum(II). *Inorg. Chem.* **2001**, *40*, 1728–1729. [CrossRef]
96. Janzen, M.C.; Jennings, M.C.; Puddephatt, R.J. Oxidative addition of mercury(II) halides and carboxylates to platinum(II): Formation of Pt–Hg covalent and donor–acceptor bonds. *Inorg. Chim. Acta* **2005**, *358*, 1614–1622. [CrossRef]
97. Anderson, L.B.; Conder, H.L.; Kudaroski, R.A.; Kriley, C.; Holibaugh, K.J.; Winland, J. Chemistry of transition-metal phosphine and phosphite complexes. 2. Preparation and properties of $XHgCo[P(OC_6H_5)_3]_3L$. *Inorg. Chem.* **1982**, *21*, 2095–2097. [CrossRef]
98. Albright, M.J.; Glick, M.D.; Oliver, J.P. Studies on main group metal-transition-metal bonded compounds.6. The structure of $\eta^5\text{-}C_5H_5(CO)_3MoHgCl$. *J. Organomet. Chem.* **1978**, *161*, 221–231. [CrossRef]
99. Bueno, C.; Churchill, M.R. Structural Studies on Some $(\eta^5\text{-}C_5H_5)M(CO)_3X$ Molecules: $(\eta^5\text{-}C_5H_5)W(CO)_3Cl$, $(\eta^5\text{-}C_5H_5)Mo(CO)_3Cl$, and $(\eta^5\text{-}C_5H_5)Mo(CO)_3HgCl$. *Inorg. Chem.* **1981**, *20*, 2197–2202. [CrossRef]
100. Cano, M.; Criado, R.; Gutierrez-Puebla, E.; Monge, A.; Pardo, M.P. Synthesis of heteronuclear carbonyl complexes $(\eta^5\text{-}C_5H_4CH_3)(CO)_3MoHgX$ (X = Cl, Br, I, SCN). Crystal structure of $(\eta^5\text{-}C_5H_4CH_3)(CO)_3MoHgCl$. *J. Organomet. Chem.* **1985**, *292*, 375–383. [CrossRef]
101. Cano, M.; Campo, J.A.; Pinilla, E.; Monge, A.; Pichon, R.; Salaün, J.-Y.; L'Haridon, P.; Szymoniak, J.; Kubicki, M.M. Effects of substitutions on cyclopentadienyl rings in complexes with molybdenum-mercury bonds. ^{95}Mo and ^{199}Hg NMR studies. *Inorg. Chim. Acta* **1995**, *228*, 251–254. [CrossRef]
102. Auvray, N.; Baul, T.S.B.; Braunstein, P.; Croizat, P.; Englert, U.; Herberich, G.E.; Welter, R. Organometallic building blocks with amino-substituted cyclopentadienyl and boratabenzene ligands for the synthesis of heterometallic complexes and clusters. *Dalton Trans.* **2006**, 2950–2958. [CrossRef]
103. Mickiewicz, M.M.; Raston, C.L.; White, A.H.; Wild, S.B. Crystal structures of Bis[tricarbonyl(η-cyclopentadienyl)molybdato(0)] mercury(II) and trans-Dicarbonyl(dimethylphenylarsine)[iodomercurio(0)](η-methylcylopentadienyl) molybdenum(II). *Aust. J. Chem.* **1977**, *30*, 1685–1691. [CrossRef]
104. Mullica, D.F.; Sappenfield, E.L.; Gipson, S.L.; Booth, A.J. Synthesis and structural analysis of trans-$Cp(CO)_2(PPh_3)WHgCl$. *Inorg. Chim. Acta* **1994**, *227*, 145–148. [CrossRef]
105. Brotherton, P.D.; Epstein, J.M.; White, A.H.; Wild, S.B. Crystal structure of (2,2′-Bipyridyl)tricarbonylchloro(chloromercurio) molybdenum-(II). *Aust. J. Chem.* **1974**, *27*, 2667–2670. [CrossRef]
106. Kergoat, R.; Kubicki, M.M.; Guerchais, J.E.; Norman, N.C.; Orpen, A.G. Bis(cyclopentadienyls) with transition metal–mercury bonds. Part 4. Formation of niobium–mercury bonds and X-ray crystal structure of $[Nb(\eta\text{-}C_5H_5)_2\{HgS_2CN(C_2H_5)_2\}_3]$. *J. Chem. Soc. Dalton Trans.* **1982**, 633–638. [CrossRef]
107. Suleimanov, G.Z.; Khandozhko, V.N.; Mekhdiev, R.Y.; Petrovskii, P.V.; Yanovskaya, I.M.; Lependina, O.L.; Kolobova, N.E.; Beletskaya, I.P. Study of the reactions of halogen and mercury halogen derivatives of metal carbonyls with samarium and ytterbium. *Russ. Chem. Bull.* **1988**, *37*, 583–588. [CrossRef]
108. Kunz, E.; Schubert, U. Übergangsmetall-Silyl-Komplexe, 27. Silylsubstituierte Hetero-Mehrkern-Komplexe durch Umsetzung der anionischen Silyl-Komplexe $[MeCpMn(CO)_2SiR_3]^-$ und $[Fe(CO)_3(PPh_3)SiR_3]^-$ mit Zink-, Cadmium- und Quecksilber-Dihalogeniden. *Chem. Ber.* **1989**, *122*, 231–234. [CrossRef]
109. Braunstein, P.; Englert, U.; Herberich, G.E.; Neuschütz, M.; Schmidt, M.U. Heterometallic complexes with borole ligands. *J. Chem. Soc. Dalton Trans.* **1999**, 2807–2812. [CrossRef]
110. Kolobova, N.E.; Valueva, Z.P.; Kazimirchuk, E.I.; Andrianov, V.G.; Struchkov, Y.T. Synthesis and some properties of tetra[η^5-cyclopentadienyldi-carbonylrheniummercury]. *Russ. Chem. Bull.* **1984**, *33*, 847–850. [CrossRef]
111. Burrell, A.K.; Clark, D.L.; Gordon, P.L.; Sattelberger, A.P.; Bryan, J.C. Syntheses and Molecular and Electronic Structures of Tris(arylimido)technetium(VI) and -(V) Complexes Derived from Successive One-Electron Reductions of Tris(arylimido)iodotechnetium(VII). *J. Am. Chem. Soc.* **1994**, *116*, 3813–3821. [CrossRef]
112. Reinhard, G.; Hirle, B.; Schubert, U. Übergangsmetall-silyl-komplexe: XLII. Einfluβ des phosphan-liganden auf bildung, struktur und stabilität der hetero-zweikernkomplexe $(CO)_3(R'_3P)(R_3Si)Fe—ML_n$ (M = Cu, Ag, Au, Hg). *J. Organomet. Chem.* **1992**, *427*, 173–192. [CrossRef]

113. Eisenmann, J.; Fenske, D.; Hezel, F. Neue phosphido- und phosphinidenverbrückte Quecksilbercluster: Die Kristallstrukturen der Mehrkernkomplexe $[Hg_3\{Fe(CO)_4\}_2X_2]$ (X = Cl, Br) (1, 2), $[Hg_{10}\{Fe(CO)_4\}_4(P^tBu)_4Cl_4]$ (3), $[Hg_{14}\{Fe(CO)_4\}_5(P^tBu)_8Cl_2]$ (4), $[SiMe_3OP^iPr_3][Hg_{12}\{Fe(CO)_4\}_7(P^tBu)_4(P^tBuSiMe_3)Br_2]$ (5), $[Hg_5\{Fe(CO)_4\}_3(P^tBu_2)_2Br_2]$ (6), $[Hg_8\{Fe(CO)_4\}_4(P_2Ph_2)_2(P^nPr_3)Cl_4]$ (7), $[Hg_8\{Fe(CO)_4\}_4(P_2Ph_2)_2(PPh_2Et)Cl_4]$ (8) und $[Hg_{10}\{Fe(CO)_4\}_6(P_2Ph_2)_2(P^nPr_3)Br_4]$ (9). *Z. Anorg. Allg. Chem.* **1998**, *624*, 1095–1104. [CrossRef]
114. Hock, H.; Stuhlmann, H. Über die Einwirkung von Quecksilbersalzen auf Eisenpentacarbonyl. *Chem. Ber.* **1928**, *61*, 2097–2101. [CrossRef]
115. Baird, H.W.; Dahl, L.F. The crystal and molecular structure of $(BrHg)_2Fe(CO)_4$. *J. Organomet. Chem.* **1967**, *7*, 503–514. [CrossRef]
116. Casey, M.; Manning, A.R. The preparation, reactions, and infrared spectra of some derivatives of bis(tricarbonylnitrosyliron)mercury. *J. Chem. Soc. A* **1970**, 2258–2261. [CrossRef]
117. Kumar, R.; Manning, A.R. Regiospecificity in the reaction of $[Fe_2(\eta\text{-}C_5H_5)_2(CO)_{4-n}(CNMe)_n]$ (n = 0–2) with mercury(II) halides. *J. Organomet. Chem.* **1981**, *216*, C61–C63. [CrossRef]
118. Granifo, J.; Vargas, M.E. The insertion of the $[M(CO)_3(NN)]$ fragments (M = Mo, W.; NN = 2,2′-bipyridine; 1,10-phenanthroline; ethylenediamine) into the Hg-X (X = Cl, Br, I, N_3, SCN) bonds of the $[\eta^5\text{-}C_5H_5Fe(CO)_2(HgX)]$ complexes. Heterotrimetallic compounds with Fe-Hg-M-X bondings. *Polyhedron* **1989**, *8*, 1471–1475. [CrossRef]
119. Bentley, G.A.; Laing, K.R.; Roper, W.R.; Waters, J.M. Preparation and crystal structure of dichloro(chloromercury)(nitrosyl)bis (triphenylphosphine)osmium(II). *J. Chem. Soc. D* **1970**, 998. [CrossRef]
120. Goodgame, D.M.L.; Slawin, A.M.Z.; Williams, D.J. Crystal structures of $[Co\{P(OPh)_3\}_4(HgX)]$, X = Cl, Br; Non-linearity of Co-Hg-X arising from intramolecular phosphorus-mercury interactions. *Polyhedron* **1987**, *6*, 543–547. [CrossRef]
121. Bonati, F.; Cenini, S.; Ugo, R. Interaction of tin(II) halides with compounds having mercury–metal bonds. *J. Chem. Soc. A* **1967**, 932–935. [CrossRef]
122. Brotherton, P.D.; Raston, C.L.; White, A.H.; Wild, S.B. Crystal structures of mercury(II) chloride and bromide addition complexes of carbonylchlorobis(triphenylphosphine)iridium(I). *J. Chem. Soc. Dalton Trans.* **1976**, 1799–1802. [CrossRef]
123. Dewhurst, R.D.; Hill, A.F.; Willis, A.C. Iridium tricarbido complexes via transmetallation with tricarbidomercurials. *Dalton Trans.* **2009**, 3384–3387. [CrossRef]
124. Hosokawa, A.; Kure, B.; Nakajima, T.; Nakamae, K.; Tanase, T. Intramolecular Metal–Metal Bond Rearrangement in a Pt_2PdHg Heterometallic Cluster Forming a Hg^I–Pd^I Covalent Bond. *Organometallics* **2011**, *30*, 6063–6066. [CrossRef]
125. Schuh, W.; Kopacka, H.; Wurst, K.; Peringer, P. Chemistry at the Sterically Shielded Mercury Centre of the $[(\eta^4\text{-pp3})PtHg]$ Fragment. *Eur. J. Inorg. Chem.* **2001**, *2001*, 2399–2404. [CrossRef]
126. Chan, W.-H.; Zhang, Z.-Z.; Mak, T.C.W.; Che, C.-M. Co-ordination chemistry of the organometallic tridentate ligand trans-$[Ru(2\text{-}Ph_2PC_5H_4N\text{-}P)_2(CO)_3]$ and crystal structures of metal complex derivatives. *J. Chem. Soc. Dalton Trans.* **1998**, 803–810. [CrossRef]
127. Xu, F.-B.; Sun, L.-J.; Xuan, Z.-A.; Zhang, W.-D.; Cheng, H.; Zhang, Z.-Z. Coordination chemistry of organometallic polydentate ligand Reactive chemistry of the tridentate ligand trans-$Fe(Ph_2PQu\text{-}P)_2(CO)_3$ [Ph_2PQu=2-diphenyl-phosphino-4-methylquinoline] and molecular structure of $[Fe(CO)_3(\mu\text{-}Ph_2PQu)_2HgI]^+[HgI_3]^-$. *Chin. J. Chem.* **2000**, *18*, 722–728. [CrossRef]
128. Kuang, S.-M.; Xue, F.; Thomas, C.W.; Mak, T.C.W.; Zhang, Z.-Z. Reaction of $M(CO)Cl(L)_2$ with mercury(II) chloride (M = Ir, Rh; L = Ph_2Ppy, $P(fur)_3$) (Ph_2Ppy = 2-(diphenylphospino)pyridine, $P(fur)_3$ = tri-(2-furyl)phosphine). *Inorg. Chim. Acta* **1999**, *284*, 119–123. [CrossRef]
129. Franciò, G.; Scopelliti, R.; Arena, C.G.; Bruno, G.; Drommi, D.; Faraone, F. IrPd, IrHg, IrCu, and IrTl Binuclear Complexes Bridged by the Short-Bite Ligand 2-(Diphenylphosphino)pyridine. Catalytic Effect in the Hydroformylation of Styrene Due to the Monodentate P-Bonded 2-(Diphenylphosphino)pyridine Ligands of trans-$[Ir(CO)(Ph_2PPy)_2Cl]$. *Organometallics* **1998**, *17*, 338–347. [CrossRef]
130. Kuang, S.-M.; Xue, F.; Zhang, Z.-Y.; Mak, T.C.W.; Zhang, Z.-Z. Metal–metal bond cleavage in the trinuclear clusters $M_3(CO)_{12-n}(Ph_2Ppy)_n$ (M = Ru, n = 3; Os, n = 1; Ph_2Ppy = 2-(diphenylphosphino)pyridine) by Lewis acids. *J. Organomet. Chem.* **1998**, *559*, 31–36. [CrossRef]
131. Baker, R.W.; Pauling, P. The crystal structure of bis(chloropyridylmercury)tetracarbonyliron, $Fe(CO)_4[HgCl(C_5H_5N)]_2$. *J. Chem. Soc. D.* **1970**, 573–574. [CrossRef]
132. Van Vliet, P.I.; Kokkes, M.; Van Koten, G.; Vrieze, K. Metal-metal bonded compounds V. Compounds with Ir(Rh)-Hg bonds containing a bridging and a chelating triazenido group, which interconvert intramolecularly. *J. Organomet. Chem.* **1980**, *187*, 413–426. [CrossRef]
133. Miu, C.-Y.; Chi, H.-H.; Chen, S.-W.; Cherng, J.-J.; Hsu, M.-H.; Huang, Y.-X.; Shieh, M. Reactions of the μ_3-sulfido triiron cluster $[SFe_3(CO)_9]^{2-}$ with functionalized organic halides and mercury salts: Selective reactivity, electrochemistry, and theoretical calculations. *New. J. Chem.* **2011**, *35*, 2442–2455. [CrossRef]

134. Shieh, M.; Tsai, Y.-C.; Cherng, J.-J.; Shieh, M.-H.; Chen, H.-S.; Ueng, C.-H.; Peng, S.-M.; Lee, G.-H. Reactivity of $[SeFe_3(CO)_9]^{2-}$ with Electrophiles: Formation of $[SeFe_2Ru_3(CO)_{14}]^{2-}$, $[SeFe_3(CO)_9(\mu\text{-HgI})]^-$, $Fe_2(CO)_6(\mu\text{-SeCHPhSe})$, and $Se_2Fe_2(CO)_6(\mu\text{-}CH_2)_2$. *Organometallics* **1997**, *16*, 456–460. [CrossRef]
135. Fernández -G, J.M.; Rosales, M.J.; Toscano, R.A. The reactivity of $[Os_3(CO)_{10}(C_2Ph_2)]$ towards phenyl mercury halides. *Polyhedron* **1988**, *7*, 2159–2163. [CrossRef]
136. Fahmy, R.; King, K.; Rosenberg, E.; Tiripicchio, A.; Tiripicchio Camellini, M. Synthesis, structure, and reactivity of mercurial derivatives of an organoruthenium cluster. *J. Am. Chem. Soc.* **1980**, *102*, 3626–3628. [CrossRef]
137. Adams, R.D.; Luo, Z.; Wong, Y.O. Bridging phenyl ligands. Unsaturated mercury-triosmium carbonyl cluster complexes containing bridging phenyl ligands. *J. Organomet. Chem.* **2015**, *784*, 46–51. [CrossRef]
138. Field, J.S.; Haines, J.R.; Meintjies, E.; Sigwarth, B.; Van Rooyen, P.H. Reduction products of dinuclear $[Rh_2Cl_2(CO)_2\{\mu\text{-}(PhO)_2PN(Et)P(OPh)_2\}_2]$. Crystal structure of $[Rh_2HgCl(\mu\text{-H})(CO)_2\{\mu\text{-}(PhO)_2PN(Et)P(OPh)_2\}_2]$. *J. Organomet. Chem.* **1984**, *268*, c43–c47. [CrossRef]
139. Adams, R.D.; Wong, Y.O. New rhenium carbonyl cluster complexes containing bridging hydrocarbyl and bridging mercury groups. *J. Organomet. Chem.* **2015**, *784*, 109–113. [CrossRef]
140. Tiripicchio, A.; Lahoz, F.J.; Oro, L.A.; Pinillos, M.T. Preparation and X-ray structure of a rhodium(III)–rhodium(I) pyrazolate complex with a mercury atom asymmetrically bridging the metal atoms. *J. Chem. Soc. Chem. Commun.* **1984**, 936–937. [CrossRef]
141. Yamaguchi, T.; Yoshiya, K. Coordination Isomers of Trinuclear Pt_2Hg Complex That Differ in Type of Metal-Metal Bond. *Inorg. Chem.* **2019**, *58*, 9548–9552. [CrossRef]
142. Della Pergola, R.; Demartin, F.; Garlaschelli, L.; Manassero, M.; Martinengo, S.; Masciocchi, N.; Sansoni, M. Chemistry of iridium carbonyl cluster complexes. Synthesis and characterization of mixed-metal carbonyl clusters via capping reactions with $HgCl_2$ and $Au(PPh_3)Cl$. Crystal structures of $[N(PPh_3)_2][Ir_6(\mu_3\text{-CO})_3(CO)_{12}(\mu_3\text{-HgCl})]\cdot 0.5C_6H_{12}$ and $[NMe_3(CH_2Ph)][Ir_6(\mu_3\text{-CO})_3(CO)_{12}[\mu_3\text{-Au}(PPh_3)]\cdot C_4H_8O$. *Organometallics* **1991**, *10*, 2239–2247. [CrossRef]
143. Ceriotti, A.; Della Pergola, R.; Garlaschelli, L.; Manassero, M.; Masciocchi, N. Au-Ir and Hg-Ir Mixed-Metal Carbonyl Clusters. Synthesis, Characterization, and Solid State Structure of $[Ir_6(CO)_{15}(AuPPh_3)_2]$ and $[Ir_6(CO)_{14}(HgCl)_2]^{2-}$. *Organometallics* **1995**, *14*, 186–193. [CrossRef]
144. Hao, L.; Manojlovic-Muir, L.; Muir, K.W.; Puddephatt, R.J.; Spivak, G.J.; Vittal, J.J.; Yufit, D. The bicluster oxidative addition as a route to bicapped hexaplatinum clusters. *Inorg. Chim. Acta* **1997**, *265*, 65–74. [CrossRef]
145. Albinati, A.; Dahmen, K.H.; Demartin, F.; Forward, J.M.; Longley, C.J.; Mingos, D.M.P.; Venanzi, L.M. A new class of planar (platinum-mercury) mixed metal clusters containing a $[Pt_3(CO)_3(PR_3)_3]$ moiety capped by two HgX units. *Inorg. Chem.* **1992**, *31*, 2223–2229. [CrossRef]
146. Gade, L.H.; Johnson, B.F.G.; Lewis, J.; McPartlin, M.; Powell, H.R. Systematic build-up of high-nuclearity osmium–mercury clusters. *J. Chem. Soc. Dalton Trans.* **1992**, 921–931. [CrossRef]
147. Bashilov, V.V.; Sokolov, V.I.; Reutov, O.A. Reactions of platinum(0) and palladium(0) complexes with mercury(II) compounds: New methods for the synthesis of organic platinum and palladium derivatives. *Russ. Chem. Bull.* **1982**, *31*, 1825–1842. [CrossRef]
148. Mednikov, E.G.; Bashilov, V.V.; Sokolov, V.I.; Slovokhotov, Y.L.; Struchkov, Y.T. Synthesis and structure of the new heteronuclear palladium-mercury cluster. *Polyhedron* **1983**, *2*, 141–144. [CrossRef]
149. Eremenko, N.K.; Kurasov, S.S.; Virovets, A.V.; Struchkov, Y.T.; Bashilov, V.V.; Sokolov, V.I. Synthesis of platinum-mercury clusters and the molecular structure of $Pt_4(HgBr)_2(\mu\text{-CO})_4(PPh_3)_4$. *Russ. Chem. Bull.* **1997**, *46*, 164–167. [CrossRef]
150. Dahmen, K.-H.; Imhof, D.; Venanzi, L.M.; Gerfin, T.; Gramlich, V. Synthesis and X-ray crystal structure of the heterometallic platinum-mercury cluster $[\{Pt_4(\mu\text{-CO})_4(PMe_2Ph)_4\}\{\mu_3\text{-HgI}\}_2]$. *J. Organomet. Chem.* **1995**, *486*, 37–43. [CrossRef]
151. Adams, R.D.; Barnard, T.S.; Cortopassi, J.E.; Zhang, L. Cluster Synthesis. 46. New Mixed-Metal Complexes of the Layer-Segregated Cluster $Pt_3Ru_6(CO)_{21}(\mu_3\text{-H})(\mu\text{-H})_3$. *Organometallics* **1996**, *15*, 2664–2667. [CrossRef]
152. Nakajima, T.; Kurai, S.; Noda, S.; Zouda, M.; Kure, B.; Tanase, T. Cyclic Trinuclear Rh_2M Complexes (M = Rh, Pt, Pd, Ni) Supported by meso-1,3-Bis[(diphenylphosphinomethyl)phenylphosphino]propane. *Organometallics* **2012**, *31*, 4283–4293. [CrossRef]
153. Casas, J.M.; Falvello, L.R.; Forniés, J.; Gomez, J.; Rueda, A. Synthesis and structural characterization of the luminescent tetranuclear complex $[NBu_4]_2[(C_6F_5)_6(\mu\text{-OH})_3Pt_3HgCl]$ with Pt-Hg bonds unsupported by covalent bridging ligands. *J. Organomet. Chem.* **2000**, *593–594*, 421–426. [CrossRef]
154. Lepetit, C.; Fau, P.; Fajerwerg, K.; Kahn, M.L.; Silvi, B. Topological analysis of the metal-metal bond: A tutorial review. *Coord. Chem. Rev.* **2017**, *345*, 150–181. [CrossRef]
155. Bridgeman, A.J.; Cavigliasso, G.; Ireland, L.R.; Rothery, J. The Mayer bond order as a tool in inorganic chemistry. *J. Chem. Soc. Dalton Trans.* **2001**, 2095–2108. [CrossRef]
156. Grimme, S.; Hansen, A.; Ehlert, S.; Mewes, J.-M. r^2SCAN-3c: A "Swiss army knife" composite electronic-structure method. *J. Chem. Phys.* **2021**, *154*, 064103. [CrossRef] [PubMed]
157. Furness, J.W.; Kaplan, A.D.; Ning, J.; Perdew, J.P.; Sun, J. Accurate and Numerically Efficient r^2SCAN Meta-Generalized Gradient Approximation. *J. Phys. Chem. Lett.* **2020**, *11*, 8208–8215. [CrossRef] [PubMed]

158. Weigend, F.; Ahlrichs, R. Balanced basis sets of split valence, triple zeta valence and quadruple zeta valence quality for H to Rn: Design and assessment of accuracy. *Phys. Chem. Chem. Phys.* **2005**, *7*, 3297–3305. [CrossRef]
159. Weigend, F. Accurate Coulomb-fitting basis sets for H to Rn. *Phys. Chem. Chem. Phys.* **2006**, *8*, 1057–1065. [CrossRef]
160. Kruse, H.; Grimme, S. A geometrical correction for the inter- and intra-molecular basis set superposition error in Hartree-Fock and density functional theory calculations for large systems. *J. Chem. Phys.* **2012**, *136*, 154101. [CrossRef]
161. Caldeweyher, E.; Ehlert, S.; Hansen, A.; Neugebauer, H.; Spicher, S.; Bannwarth, C.; Grimme, S.A. Generally applicable atomic-charge dependent London dispersion correction. *J. Chem. Phys.* **2019**, *150*, 154122. [CrossRef]
162. Cossi, M.; Rega, N.; Scalmani, G.; Barone, V. Energies, structures, and electronic properties of molecules in solution with the C-PCM solvation model. *J. Comput. Chem.* **2003**, *24*, 669–681. [CrossRef]
163. Neese, F. The ORCA program system. *WIREs Comput. Mol. Sci.* **2012**, *2*, 73–78. [CrossRef]
164. Neese, F. Software update: The ORCA program system—Version 5.0. *WIREs Comput. Mol. Sci.* **2022**, *12*, e1606. [CrossRef]
165. Lu, T.; Chen, F. Multiwfn: A multifunctional wavefunction analyser. *J. Comput. Chem.* **2012**, *33*, 580–592. [CrossRef]
166. Hezel, F.; Fenske, D.; Eisenmann, J.; Wetzel, T. Synthese und Kristallstructuren neuer phosphorverbrückter bimetallischer Cluster der Elemente Quecksilber und Eisen. *Z. Anorg. Allg. Chem.* **2000**, *626*, 290–301. [CrossRef]